bioRxiv preprint doi: https://doi.org/10.1101/2022.04.08.487612; this version posted April 10, 2022. The copyright holder for this preprint (which was not certified by peer review) is the author/funder, who has granted bioRxiv a license to display the preprint in perpetuity. It is made available under aCC-BY-NC-ND 4.0 International license.

The *GUN* mutants: new weapons to unravel ascospore germination regulation in the model fungus *Podospora anserina*

Alexander Demoor, Isabelle Lacaze, Roselyne Ferrari, Christophe Lalanne, Philippe Silar and Sylvain Brun*#

Université Paris Cité, Laboratoire Interdisciplinaire des Energies de Demain - UMR 8236, 5 rue Marie-Andrée Lagroua-Weill-Hall, 75205 Paris cedex 13, France

*: **Correspondence to Dr. Sylvain Brun:** sylvain.brun@u-paris.fr
#: **Present address:** Université Paris Cité, Institut Jacques Monod - UMR 7592, team Polarity & Morphogenesis, 15 rue Hélène Brion, 75205 Paris CEDEX 13

Key words: ascospore germination; Carnitine-acetyl transferase, peroxisomes; mitochondria; *Podospora anserina*; fungi

Running title: characterization of the *GUN1*^{SG} mutant in *P. anserina*

bioRxiv preprint doi: https://doi.org/10.1101/2022.04.08.487612; this version posted April 10, 2022. The copyright holder for this preprint (which was not certified by peer review) is the author/funder, who has granted bioRxiv a license to display the preprint in perpetuity. It is made available under aCC-BY-NC-ND 4.0 International license.

Abstract

In *Podospora anserina* as in many other *ascomycetes*, ascospore germination is a regulated process that requires breaking of dormancy. Despite its importance in survival and dispersal, ascospore germination in filamentous fungi has been poorly investigated and little is known about its regulation and genetic control. We have designed a positive genetic screen that led to the isolation of mutants showing uncontrolled germination, the *GUN* mutants. In this paper, we report on the characterization of *GUN1*^{SG}. We show that *GUN1*^{SG} is mutated in *Pa_6_1340,* the ortholog of *Magnaporthe oryzae Pth2,* which encodes a Carnitine-acetyltransferase (CAT) involved in the shuttling of acetyl-CoA between peroxisomes and mitochondria and which is required for appressorium-development. Bioinformatic analysis revealed that the mutated residue (I441) is highly conserved among the *Fungi*, and that the mutation has a deleterious impact on the protein function. We show that GUN1 is essential for ascospore germination and that the protein is localized both in mitochondria and in peroxisomes. Finally, epistasis studies allowed us to place *GUN1* upstream of the *PaMpk2* MAPK pathway and the *PaNox2*/*PaPls1* complex in the regulation of ascospore germination. The identification of *GUN1*, the ortholog of *Pth2,* in ascospore germination, strengthens the idea of a common genetic regulation governing both appressorium development and melanized ascospore germination. In addition, we characterize the second CAT encoded in *P. anserina* genome, *Pa_3_7660*/*GUP1,* and we show that the function of both CATs is conserved *in P. anserina*.

bioRxiv preprint doi: https://doi.org/10.1101/2022.04.08.487612; this version posted April 10, 2022. The copyright holder for this preprint (which was not certified by peer review) is the author/funder, who has granted bioRxiv a license to display the preprint in perpetuity. It is made available under aCC-BY-NC-ND 4.0 International license.

Introduction

Fungi are eukaryotic microorganisms able to resist adverse environments and disseminate through the formation of asexual (mitospores) or sexual spores (meiospores). Representing the final product of sexual reproduction, meiospores ensure survival, dissemination and carry genetic diversity, promoting adaptation in changing environments (Hoekstra, 2005). Spore germination is a crucial step in fungal life cycle, and its successful completion is thus essential for survival and spread. Conidial germination represents the starting point of infection for important pathogenic species such as *Aspergillus fumigatus* or *Magnaporthe oryzae,* and its regulation has therefore been widely studied (Baltussen et al., 2020; Osherov and May, 2001). By contrast, little is known about the regulation of ascospore germination, although ascospores are the key dispersal propagule for many other important pathogenic species such as *Leptosphaeria maculans*, the main pathogen for oilseed rape cultures (Daverdin et al., 2012; Howlett et al., 2001). Although conidial germination and ascospore germination share some morphological similarities, several studies have demonstrated that their regulation is different (Trapero-Casas and Kaiser, 2007). *Podospora anserina*, a saprotrophic coprophilous *ascomycete* from the *sordariales* order, emerges as an excellent genetic model system to study ascospore germination. *P. anserina* produces asexual spermatia that are unable to germinate, as well as ascospores that represent the only germinating spores in this fungus. This species forms after fertilization pear-shaped fruiting bodies called perithecia, each harboring a few hundred to a thousand ascospores, generally embedded in groups of four inside asci (Silar, 2020). The melanized ascospores of *P. anserina* are in a dormant state and require a stimulus in order to germinate. *P. anserina* is a coprophilous fungus reported to grow preferentially on herbivores' dung. Indeed, in the wild, the breaking of dormancy of *P. anserina* ascospores is usually triggered by the passage through herbivores digestive tract, leading to germination on dung. This stimulus is reproduced in laboratory conditions, by placing the ascospores on a germination medium (Silar, 2020). In *P. anserina*, ascospore germination takes place in several steps: i) the activation by the stimulus (dormancy breaking), ii) formation of the germination pore at the apex of the spore (opposite to the primary appendage), iii) extrusion of a germination peg/bubble from which one or several (often two) germinating hyphae emerge.

It was shown that both H_2O_2 and O_2^- Reactive Oxygen Species (ROS) are produced during ascospore germination in *P. anserina*, suggesting that ROS play an important role at this stage (Malagnac et al., 2004). Knock-out of the superoxide (O_2^-**)** producing enzyme Nicotinamide-Adenine-Dinucleotide-Phosphate (NADPH) oxidase *PaNox2* encoding gene, of the *PaPls1* tetraspanin encoding gene as well as the regulatory subunit *PaNoxR*, leads to an almost complete abolishment of ascospore germination (Brun et al., 2009; Lambou et al., 2008; Malagnac et al., 2004). Remarkably, mutations (or deletions)

bioRxiv preprint doi: https://doi.org/10.1101/2022.04.08.487612; this version posted April 10, 2022. The copyright holder for this preprint (which was not certified by peer review) is the author/funder, who has granted bioRxiv a license to display the preprint in perpetuity. It is made available under aCC-BY-NC-ND 4.0 International license.

of the orthologs of *PaNox2* and *PaNoxR* genes lead to loss-of-ascospore germination ability, in both model species *Sordaria macrospora* and *Neurospora crassa*, highlighting the conservation of Nox2/B, and NoxR functions in the regulation of ascospore germination (Cano-Dominguez et al., 2008; Dirschnabel et al., 2014). Strikingly, the NADPH oxidase complexes Nox1/A, Nox2/B, NoxR and Pls1 are required for appressorium functioning in the plant pathogenic fungus *M. oryzae* (Lambou et al., 2008; Ryder et al., 2013, 2019). Considering that the ascospores in *P. anserina* and the appressorium in *M. oryzae* are both melanized structures, we have hypothesized that, similar components and in particular the Nox2/B-Pls1-NoxR complex regulate cellular processes such as the formation of the pore through which arise the penetration peg in *M. oryzae* and the germination peg in *P. anserina* (Brun and Silar, 2010; Malagnac et al., 2008).

The same hypothesis applies to the Mitogen-Activated-Protein-Kinase (MAPK) pathway *PaMpk2/MoPmk1/ScFus3* involved in appressorium development in *M. oryzae* as well as in ascospore germination in *P. anserina* (Lalucque et al., 2012; Widmann et al., 1999; Xu et al., 1998). We have shown that loss-of-function of each of the three kinases of the MAPK cascade in *P. anserina*, *i.e., PaTlk2*, *PaMkk2* and *PaMpk2*, abolishes ascospore germination. Conversely, the activation of the pathway in the constitutively active *PaMkk2^{c}* mutant, leads to spontaneous germination of ascospores (Lalucque et al., 2012). In *N. crassa*, mutants of MAK-2, the ortholog of Fus3/PaMpk2 and mutants of pp-1/Ste12, the downstream transcription factor of the cascade, show almost complete lack of ascospore germination (Li et al., 2005; Pandey et al., 2004). In addition, Knock-Out of the *Ste12* ortholog in *S. macrospora* also impairs ascospore germination (Nolting and Pöggeler, 2006). Interestingly, these three species harbor melanized ascospores that require a stimulus to germinate and this raises questions as to the role of this pigment during spore germination.

As in other fungi, melanin in *P. anserina* is synthesized through an enzymatic cascade, starting with the PaPks1 Polyketide Synthase. Inactivation of this key enzyme results in total inability to produce melanin in hyphae, perithecia and ascospores, as observed in the *PaPks1^{193}* and the *ΔPaPks1* null mutants (Coppin and Silar, 2007; Gautier et al., 2021; Langfelder et al., 2003). Remarkably, non-melanized ascospores in the *PaPks1^{193}* mutant escape from dormancy and germinate spontaneously. Since the presence of melanin in cell wall contributes to its rigidity (Gómez and Nosanchuk, 2003), it is assumed that lack of melanin weakens the ascospore cell wall, leading to “accidental”, uncontrolled germination. In line with this, culturing and crossing *P. anserina* on medium containing the fungicide Tricyclazole, an inhibitor of melanin production in fungi, allows ascospores bearing mutations in genes essential for germination such as *PaNox2*, *PaNoxR*, *PaPls1 or PaMpk2* to spontaneously germinate (Brun et al., 2009; Coppin and Silar, 2007; Lalucque et al., 2012; Lambou et al., 2008; Malagnac et al.,

bioRxiv preprint doi: https://doi.org/10.1101/2022.04.08.487612; this version posted April 10, 2022. The copyright holder for this preprint (which was not certified by peer review) is the author/funder, who has granted bioRxiv a license to display the preprint in perpetuity. It is made available under aCC-BY-NC-ND 4.0 International license.

2004). It is worth noting that these non-melanized ascospores are fragile and lose viability if manipulated (when moved with a needle for harvesting for instance).

A defect in ascospore melanization and germination is also observed in mutants of peroxisome biogenesis, peroxisomal β-oxidation and mitochondrial β-oxidation. In these mutants, depletion in acetyl-Coenzyme A (acetyl-CoA) the direct product of β-oxidation and the main precursor for melanin biosynthesis is supposed to account for both defects (Berteaux-Lecellier et al., 1995; Boisnard et al., 2009; Bonnet et al., 2006; Peraza-Reyes et al., 2008). Peroxisomes are organelles of fundamental importance in particular for fungal pathogenesis (Asakura et al., 2006; Imazaki et al., 2010; Peraza-Reyes et al., 2011). In *M. oryza*e, mutants affected in peroxisomal β-oxidation and acetyl-CoA metabolism show: defects in appressorium development, appressorium demelanization and lack of pathogenicity (Chen et al., 2016; Kretschmer et al., 2012; Wang et al., 2007). Besides, the Carnitine-acetyl transferase (CAT) *Pth2* mutant was isolated in a forward genetic screen designed to uncover pathogenicity mutants in *M. oryzae*, underlining the central role of acetyl-CoA metabolism during *M. oryzae* infection (Bhambra et al., 2006; Ramos-Pamplona and Naqvi, 2006; Sweigard et al., 1998).

Despite the lack of knowledge on ascospore germination, this process has never been subjected to any dedicated genetic screening. In this paper, we describe the first genetic screening of ascospore germination mutants. Previous observations have shown that a negative genetic screening of mutants defective for ascospore germination i) is time-consuming compared to positive screening, ii) may lead to the isolation of mutants nonspecifically affected in any kind of cellular processes eventually leading to lack of viability/germination of ascospores and iii) brings intrinsic issues in genetic analysis since these non-germinating mutants are blocked in their sexual/life cycle. With that in mind, we have designed a direct genetic screen aiming at isolating spontaneous germination mutants in the wild-type *P. anserina* strain normally showing controlled germination. Moreover, with the aim to isolate mutants of the *PaNox2-PaPls1* pathway, we have also screened for suppressors of *ΔPaNox2* and *ΔPaPls1*, for which germination was restored. In this paper, we describe the *Germination UNcontrolled One* (*GUN1*^{SG}) mutant, we identify and we characterize the gene affected as well as its paralogue the "*GUN1 Paralogue One"* gene (*GUP1*). The functional analysis of both genes show that *GUN1* codes for the ortholog of the *M. oryzae Pth2/Crat1* CAT (*CAT2* in *Saccharomyces cerevisiae*; *AcuJ* in *Aspergillus nidulans*), *GUP1* codes for the ortholog of the *FacC* CAT in *A. nidulans* and *Crat2* in *M. oryzae* (Bhambra et al., 2006; Hynes et al., 2011; Ramos-Pamplona and Naqvi, 2006; van Roermund et al., 1999) and only GUN1 is important for ascospore germination and melanization.

bioRxiv preprint doi: https://doi.org/10.1101/2022.04.08.487612; this version posted April 10, 2022. The copyright holder for this preprint (which was not certified by peer review) is the author/funder, who has granted bioRxiv a license to display the preprint in perpetuity. It is made available under aCC-BY-NC-ND 4.0 International license.

Results

Isolation of *Germination Uncontrolled-GUN* mutants

In *P. anserina*, wild-type ascospores are dormant and do not germinate on standard M2 medium. They require a stimulus to germinate (see movie S1 for wild-type germination), provided in laboratory conditions in the specific germination G medium, supplemented with yeast extract (YE) to increase germination rate (Silar, 2013). Rather than screening for mutants unable to germinate, we set up a positive genetic screen allowing isolation of mutants producing spontaneously germinating ascospores on M2 medium. In parallel, we screened for suppressors of the germination defect of the *ΔPaNox2* and *ΔPaPls1* mutant strains (Malagnac et al., 2004, 2008) using the same protocol. Auto-fertile (*mat+/mat-*) mycelia of the *S*, *ΔPaNox2* and *ΔPaPls1* strains were exposed to UV mutagenesis and mutants producing spontaneously germinating ascospores on standard M2 medium were isolated (see Figure S1 and Mat. & Met.). Mutant screening allowed recovery of 22 suppressors of *ΔPaNox2*, 16 suppressors of *ΔPaPls1*, and 19 mutants from the *S* strain, all of them producing ascospores spontaneously germinating on standard M2 medium (Table S1). Genetic analysis of these mutants revealed that for all of them, the mutant phenotype was controlled by a single locus. We then checked the germination process in these 57 mutants by microscopic analysis. For all the suppressors of *ΔPaNox2* and *ΔPaPls1,* and 13 mutants of the *S* strain, ascospore germination was morphologically abnormal. In these mutants, we could observe germination through the primary appendage. This latter selection was important to possibly discard structural mutants in which the ascospore cell wall was impaired, leading to "accidental" germination or mutants in which the cell constituting the primary appendage failed to degenerate. Indeed, in *P. anserina* the cell constituting the primary appendage degenerates, otherwise, a germ tube arises from this cell, leading to spontaneous germination. Only 6 of the mutants isolated from the wild-type *S* strain showed morphologically "normal" germination proceeding through the germination pore (Table S1 & movie S1). We speculated that these six mutants represent mutants of genes involved in the signalling pathway that controls germination and were named *GUNx*^{SG} for *Germination Uncontrolledx*$^{Spontaneous\ Germination}$ where x stands for the mutant number. Among these mutants, one had the particular characteristic to germinate on agar plates devoid of carbon and nitrate sources while the five others did not (data not shown). We therefore started the characterization of this mutant that we named *GUN1*^{SG}. This mutant differentiated ascospores with normal shape (Figure 1A), visually normal melanization and spontaneous germination through the germination pore (Figure 1B). We determined the germination rate of this mutant on M2 medium, as well as on G+YE medium, and compared it to the wild-type. Throughout our experiments, we never observed germination of wild-type ascospores when sown

bioRxiv preprint doi: https://doi.org/10.1101/2022.04.08.487612; this version posted April 10, 2022. The copyright holder for this preprint (which was not certified by peer review) is the author/funder, who has granted bioRxiv a license to display the preprint in perpetuity. It is made available under aCC-BY-NC-ND 4.0 International license.

onto M2 medium. In contrast, when *GUN1*^{SG}/*GUN1*^{SG} heterokaryotic ascospores were transferred onto M2 medium to estimate germination rate, 54/100 germinated. In the same experiment, 94/100 germinated on G+YE, a comparable rate to *WT* ascospores (92/100). Once germination was initiated, development of the mycelium produced by the *GUN1*^{SG} mutant was identical to the wild-type: the *GUN1*^{SG} mutant showed wild-type vegetative phenotype, growth rate, fertility, ascospore production, appressorium development and cellophane breaching (Figure 2, S2 & Table 2).

GUN1 encodes a Carnitin-acetyltransferase (CAT)

The gene mutated in *GUN1*^{SG} was identified through whole-genome sequencing. To that end, this mutant was backcrossed five times with the wild-type strain beforehand in order to eliminate most of the mutations generated during UV mutagenesis but not genetically linked to the mutation responsible for the mutant phenotype. The analysis of *GUN1*^{SG} whole-genome sequence revealed the presence of six silent mutations, and three missense mutations, one in *Pa_1_13700*, which encodes a putative protein of unknown function, another in *Pa_5_7800*, encoding a putative phosphoketolase and the last one in the *Pa_6_1340* CDS, where an isoleucine was changed into an asparagine (I441N), caught our attention (Figure 3). RNA-seq data indicated that *Pa_6_1340* was strongly induced (Fold Change = 56) during ascospore germination, emphasizing the involvement of this gene during ascospore germination (Demoor, unpublished data). This CDS encodes a putative peroxisomal/mitochondrial Carnitine-acetyltransferase (CAT) of 643 amino acids (Masterson and Wood, 2000; Seccombe and Hahn, 1980; Strijbis and Distel, 2010; Strijbis et al., 2010). Homologs of this gene have previously been studied in *S. cerevisiae*, *Aspergillus nidulans, Giberella zeae, Sclerotinia sclerotiorum* and *M. oryzae* where they are involved in acetate/acetyl-CoA metabolism and more particularly in pathogenicity and appressorium development in the phytopathogenic species mentioned (Bhambra et al., 2006; Hynes et al., 2011; Liberti et al., 2013; Ramos-Pamplona and Naqvi, 2006; Son et al., 2012). Regarding the role of acetate and peroxisomes in the control of germination in *P. anserina*, and given the induction of *Pa_6_1340* during ascospore germination, this gene emerged as a particularly good candidate for further study.

In order to explore the role of *Pa_6_1340* in the ascospore germination process, a gene replacement was performed, in which the *Pa_6_1340* CDS was substituted by a hygromycin B resistance marker (Figure S3). The gene disruption construct was introduced into a *Δmus51::phleoR* strain impaired for NHEJ (El-Khoury et al., 2008). Two independent hygromycin B-resistant [hygR] transformants were obtained. In order to purify *ΔPa_6_1340::hygR* from the *Δmus51::phleoR* mutation, we crossed both

bioRxiv preprint doi: https://doi.org/10.1101/2022.04.08.487612; this version posted April 10, 2022. The copyright holder for this preprint (which was not certified by peer review) is the author/funder, who has granted bioRxiv a license to display the preprint in perpetuity. It is made available under aCC-BY-NC-ND 4.0 International license.

primary transformants with the *S* strain. Strikingly, we observed partially demelanized ascospores in the progeny of both crosses. Furthermore, when homokaryotic ascospores were sown on G+YE germination medium, only half of the progeny germinated, and those were only [hygS] melanized ascospores. This suggested that the [hygR] *ΔPa_6_1340::hygR* ascospores were the partially demelanized ones and that they were not able to germinate. These crosses were repeated on M2 medium supplemented with Tricyclazole, a fungicide impairing melanin synthesis and provoking spontaneous germination of ascospores in *P. anserina* (Coppin and Silar, 2007). We collected ascospores directly projected on M2 medium supplemented with hygromycin B and we isolated [hygR] germinating thalli. These thalli were fragmented and homokaryotic [hygR, phleoS] *ΔPa_6_1340::hygR* strains of each mating type were purified. Deletion of *Pa_6_1340* CDS in these strains was verified by Southern Blot analysis (Figure S3) and mutant phenotypes were characterized. In homozygous *ΔPa_6_1340::hygR* X *ΔPa_6_1340::hygR* crosses ascospores exhibited demelanization and completely lost their ability to germinate on G+YE medium, a phenotype opposite to that of *GUN1*^{SG} (Figure 1). Genetic analyses of heterokaryotic ascospores showed that this phenotype due to *ΔPa_6_1340::hygR* deletion was recessive and that *ΔPa_6_1340::hygR* segregated with a Second Division Segregation (SDS) rate of 55% (see Mat. & Met.). Fertility in *ΔPa_6_1340::hygR* was affected too: perithecium production in a *ΔPa_6_1340::hygR* X *ΔPa_6_1340::hygR* cross was slightly reduced and ascospore production was significantly diminished compared to a wild-type cross (Figure S2). It has been shown that the formation of the appressorium in *M. oryzae* and the germination of melanized ascospores in *P. anserina* are two processes sharing common regulatory elements (Malagnac et al., 2008). We found that in the *ΔPa_6_1340::hygR* mutant, breaching of cellophane (a process involving appressorium development in *P. anserina*) was delayed compared to the wild-type (Table 2). However, microscopic observations did not detect any morphological defect of appressorium development (data not shown). Importantly, introduction of the wild-type allele of *Pa_6_1340* carried on the *pGUN1* plasmid (see Mat. & Met.) into the *ΔPa_6_1340::hygR* genome restored wild-type phenotypes thus showing that the deletion of *Pa_6_1340* was responsible for the mutant phenotypes (Figure 1, 2, 4 & S2).

Finally, we addressed the question whether the phenotypes in the *GUN1*^{SG} mutants were due to the I441N mutation in *Pa_6_1340* by testing whether *ΔPa_6_1340::hygR* and *GUN1*^{SG} are alleles of the same gene in a complementation test. In a first step, we genetically determined that spontaneous germination in *GUN1*^{SG} was a recessive trait, a prerequisite for the complementation test. These genetic analyses also showed that *GUN1*^{SG} segregated with a SDS rate of 54%, very similar to that of *ΔPa_6_1340::hygR* (55%), suggesting that *ΔPa_6_1340::hygR* and *GUN1*^{SG} could be allelic (see Mat. & Met.). We then crossed *GUN1*^{SG} with *ΔPa_6_1340::hygR* reasoning that if *ΔPa_6_1340::hygR* and *GUN1*^{SG} are allelic, no functional complementation in heterokaryotic ascospores in SDS asci is expected

bioRxiv preprint doi: https://doi.org/10.1101/2022.04.08.487612; this version posted April 10, 2022. The copyright holder for this preprint (which was not certified by peer review) is the author/funder, who has granted bioRxiv a license to display the preprint in perpetuity. It is made available under aCC-BY-NC-ND 4.0 International license.

for the spontaneous germination of *GUN1^{SG}*: *ΔPa_6_1340::hygR/GUN1^{SG}* ascospores germinate spontaneously on M2 medium; in contrast, if *GUN1^{SG}* and *ΔPa_6_1340::hygR* are not allelic, functional complementation leading to restoration of wild-type phenotype is expected: *Pa_6_1340::hygR/Pa_6_1340 GUN1^{SG}/GUN1* heterokaryotic ascospores in SDS asci germinate as wild-type. We observed that heterokaryotic ascospores in SDS asci germinated spontaneously on M2 medium showing that *GUN1^{SG}* and *ΔPa_6_1340* were allelic (no complementation). This demonstrated that *Pa_6_1340* was the gene mutated in the *GUN1^{SG}* mutant responsible for the spontaneous germination phenotype. We therefore named *Pa_6_1340, GUN1*. This evidence was confirmed when we showed that the *GUN1^{SG}* mutant was also complemented by ectopic integration of a wild-type copy of *Pa_6_1340*/*GUN1* carried by the pGUN1 plasmid (Table 3 and Mat. & Met.).

P. anserina possess two CATs

A BLASTP search on the *P. anserina* predicted CDS database (http://podospora.i2bc.paris-saclay.fr/) identified a second CAT encoded by the *Pa_3_7660* putative CDS. Compared to GUN1, this putative enzyme did not harbor any localization signal. Similarly to other fungi, *P. anserina* may be endowed with two types of CAT, one located in peroxisomes and in mitochondria (GUN1) and one remaining in the cytoplasm (Pa_3_7660). To confirm this hypothesis, we undertook a phylogenetical analysis of CATs in *Eumycetes* and searched the homologs of *GUN1* in the genome sequence of representative fungal species (see Mat. & Met.). In these species, 2 CATs were always identified, except for *S. cerevisiae* in which three CATs were identified as previously shown (Swiegers et al., 2001). The protein sequences were aligned and the corresponding phylogenetic tree was built (Figure S4). The phylogeny of CATs in *Eumycetes* clearly indicated that there are 2 main types of CATs in fungi: the putative peroxisomal/mitochondrial CAT including GUN1, *A. nidulans* AcuJ and *M. oryzae* Pth2/Crat1 and the putative "cytoplasmic" CATs including *P. anserina* Pa_3_7760, *A. nidulans* FacC and *M. oryzae* Crat2. Careful analysis of protein sequences indicated that proteins of the former type all contained the appropriate sequence signals to locate in peroxisomes and in mitochondria. In addition, search for orthologs through OrthoDB (Kriventseva et al., 2019) did not identify orthologs for either *GUN1* or *Pa_3_7760* in plants nor in bacteria.

Pa_3_7760 putative CDS was renamed *GUP1* for *GUN1 Paralog 1*. With the aim of determining the function of this second CAT and to assess its role in ascospore germination, we undertook a targeted gene disruption of *GUP1*. The *Pa_3_7660* CDS was replaced by a phleomycin resistance marker through homologous recombination in a *Δmus51::genR* strain (see Mat. & Met. and Figure S5). The

bioRxiv preprint doi: https://doi.org/10.1101/2022.04.08.487612; this version posted April 10, 2022. The copyright holder for this preprint (which was not certified by peer review) is the author/funder, who has granted bioRxiv a license to display the preprint in perpetuity. It is made available under aCC-BY-NC-ND 4.0 International license.

ΔGUP1 strain was purified from the *Δmus51* mutation by crossing primary transformants with the wild-type *S* strain followed by the selection of [phleoR, genS] homokaryotic ascospores of the *ΔGUP1* genotype in the progeny. *ΔGUP1* ascospores had no melanization defect and germinated on G+YE medium as the wild-type. Importantly, when *ΔGUP1* homokaryotic ascospores were sown on M2 medium, no spontaneous germination was observed, leading us to conclude that *GUP1* deletion had no effect on ascospore melanization and germination in *P. anserina*. In addition, the *ΔGUP1* strain differentiated wild-type mycelium and exhibited wild-type fertility, ascospore production, (Figure 2 & S2) appressorium development and cellophane breaching (data not shown). We then constructed the *ΔGUN1 ΔGUP1* double mutant (see Mat. & Met.) and we observed that *ΔGUN1 ΔGUP1* homokaryotic ascospores exhibited impaired melanization and lack of germination similarly to the *ΔGUN1* ascospores.

GUN1 and GUP1 functions are conserved in fungi

Previous studies in fungi have revealed that CATs play an important role in primary metabolism and carbon source utilization. In particular, it has been shown that K.O strains of the cytoplasmic CAT do not grow on acetate whereas mutant strains of the peroxisomal/mitochondrial CAT do not grow on acetate and on media containing fatty acids such as oleic acid (Bhambra et al., 2006; Hynes et al., 2011; Liberti et al., 2013; Son et al., 2012; Swiegers et al., 2001). To assess the role of GUN1 and GUP1 in carbon source utilization, we have tested growth of the different mutant strains on acetate and oleic acid. As shown in Figure 2, the wild-type *S* strain was able to grow on all the tested media, including the Tween 40 control (Tween 40 is necessary to solubilize oleic acid), indicating that *P. anserina* was able to use this detergent as a carbon source. Remarkably, $GUN1^{SG}$ as well as the $GUN1^{SG}$ *pGUN1* complemented strain grew as the wild-type. The *ΔGUN1*, *ΔGUP1* and the double *ΔGUN1 ΔGUP1* mutants grew as wild-type on dextrin (M2 medium), *ΔGUN1* and *ΔGUN1 ΔGUP1* exhibited slightly reduced growth on Tween 40, almost no growth on oleic acid and no growth on acetate whereas *ΔGUP1* growth was impaired only on acetate. *ΔGUP1 pGUP1* had restored wild-type growth on acetate indicating that wild-type *GUP1* complemented *ΔGUP1* deletion. This confirmed that *GUP1* function was required in *P. anserina* on acetate. Similarly, wild-type growth was restored on Tween 40 and oleic acid in both *ΔGUN1 pGUN1* and *ΔGUN1 ΔGUP1 pGUN1* complemented strains indicating that *GUN1* function was required for Tween 40 and oleic acid utilization. These data also showed that *ΔGUN1* was epistatic on *ΔGUP1* when *P. anserina* was grown on Tween 40 and on oleic acid. Strikingly, both the *ΔGUN1* and the *ΔGUN1 ΔGUP1* strains could grow on Tween 40 but not on oleic acid medium although this latter contained the same amount of Tween 40 (0,5%) (see Mat. & Met.). This suggested

bioRxiv preprint doi: https://doi.org/10.1101/2022.04.08.487612; this version posted April 10, 2022. The copyright holder for this preprint (which was not certified by peer review) is the author/funder, who has granted bioRxiv a license to display the preprint in perpetuity. It is made available under aCC-BY-NC-ND 4.0 International license.

that impaired growth on oleic acid for *ΔGUN1* and *ΔGUN1 ΔGUP1* strains was due to a toxic effect of oleic acid in these mutant strains. Overall, these data showed that the roles of both main types of CATs were conserved in *P. anserina*: CATs of the AcuJ/Pth2/Crat1/GUN1-type are required for growth on acetate as well as on long chain fatty acids whereas CATs of the FacC/Crat2/GUP1-type are required for growth on acetate.

Structure prediction analysis of *GUN1^{SG}* loss-of-function

MAFFT alignment with the protein sequences encoded by the fungal orthologs of *GUN1*, including the ortholog from *Homo sapiens* revealed that the isoleucine 441 mutated in the *GUN1^{SG}* mutant (I441N) was highly conserved in *Eumycota*: it is conserved in *Pezizomycotina*, *Saccharomycotina*, *Mucoromycota* and in *Basidiomycota* (Figure S6). Using I-TASSER, we realized 3D structure prediction of GUN1, and we compared it to the 3D structure of the murine CAT (34% identity). As can be seen in Figure 3C, the overall structure of both enzymes was well conserved, showing that the 3D-modelling of GUN1 was congruent. Based on this GUN1 3D-model, we could localize the Isoleucine 441 near the extremity of an α-helix. Since hydrophobicity of amino acids is paramount in α-helix formation, we wondered whether the substitution of aliphatic isoleucine 441 by polar asparagine could destabilize the α-helix and/or the whole protein. We determined the Gibbs free-energy Gap (ΔΔG) provoked by the I441N substitution in GUN1^{SG} with STRUM (Funahashi et al., 2003). The calculated ΔΔG of 2.11 kcal.mol^{-1} was indeed indicative of a destabilization of the GUN1^{SG} mutant protein but this low ΔΔG value (<6 kcal.mol^{-1}) was rather indicative of a local destabilization of the protein rather than a complete destabilization (Faure and Koonin, 2015). In line with this, we did not notice any stability issues in both chimera reporters GUN1^{SG}-mCherry and GUN1^{SG}-mCherry-AKI compared to GUN1-mCherry and GUN1-mCherry-AKI respectively, in our microscopic observations (see later). We also used the PROVEAN analysis tool to determine the impact of the I441N substitution on GUN1 function. Accordingly to the recessive nature of the *GUN1^{SG}* mutation, the calculated PROVEAN score of -6.63, far below the predefined cutoff of -2.5 was predictive of a "deleterious" loss-of-function effect of the I441N substitution on GUN1 function (Choi and Chan, 2015; Choi et al., 2012).

CAT activity decreases in *GUN1^{SG}* and *ΔGUN1*

We measured the CAT activity in different mutant strains in protein extracts from mycelium grown on M2 medium (Figure 4). It is worth to mention that we failed to measure CAT activity in ascospores and we could only obtain reliable results in mycelia (see Mat. & Met.). Compared to the wild-type, CAT

bioRxiv preprint doi: https://doi.org/10.1101/2022.04.08.487612; this version posted April 10, 2022. The copyright holder for this preprint (which was not certified by peer review) is the author/funder, who has granted bioRxiv a license to display the preprint in perpetuity. It is made available under aCC-BY-NC-ND 4.0 International license.

activity in mycelium was greatly reduced in *ΔGUN1, ΔGUN1 ΔGUP1* as well as the in *GUN1^{SG}* mutants. Significantly, CAT activity was restored to the wild-type level in the *ΔGUN1 pGUN1* and *ΔGUN1 ΔGUP1 pGUN1* complemented strains confirming that lack of *GUN1* was responsible for reduced CAT activity. In the complemented *GUN1^{SG} pGUN1* strain, the CAT activity was even higher than in the wild-type pointing to a role of CAT activity increase in the restoration of wild-type phenotype in *GUN1^{SG} pGUN1*. Interestingly, CAT activity in *ΔGUP1* was similar to wild-type CAT activity, a result in agreement with previous observations in *M. oryzae* showing that CAT activity in *ΔCrat2* (the ortholog of *GUP1*) mutants was not altered (Ramos-Pamplona and Naqvi, 2006). These results showing a decreased CAT activity in *GUN1^{SG}* and hence a loss-of–function of GUN1^{SG} were congruent with the modelized "deleterious" effect of the I441N mutation on GUN1^{SG} function and the recessivity of the *GUN1^{SG}* phenotype. However, the fact that similar reduced CAT activity was measured in *GUN1^{SG}* and *ΔGUN1* ($P<0.05$) suggested that the CAT activity measured in mycelium did not account for the difference in phenotype between the *GUN1^{SG}* and *ΔGUN1* mutants (*i.e.,* germination and melanization of ascospores, acetate and acid oleic growth).

Subcellular localization of GUN1 and GUN1^{SG} proteins

Previous studies carried out on GUN1-type CATs in other fungal species have revealed that these enzymes could be localized in peroxisomes and in mitochondria (Hynes et al., 2011; Zhou and Lorenz, 2008). Analysis of GUN1 protein sequence using wolfPSORT indicated that GUN1 probably located in both peroxisomes and mitochondria. Accordingly, scanning GUN1 protein sequence with MitoFates allowed us to identify a Mitochondrial Targeting Sequence (MTS) and we manually identified the "AKI" tripeptide at the C-terminal end of the protein sequence as a type 1 Peroxisomal Targeting Sequence (PTS1) (Brocard and Hartig, 2006) (Figure 3). In order to investigate GUN1 subcellular localization as well as the impact of the *GUN1^{SG}* mutation on its subcellular localization, we tagged both GUN1 and GUN1^{SG} with mCherry and with mCherry-AKI, a modified mCherry version bearing the putative PTS1 peroxisome targeting signal of GUN1 in C-terminus (Figure 3). As previously mentioned, *GUN1* is specifically induced in ascospores during germination (Demoor, unpublished data). To ensure that expression of the fusion proteins was under the control of the native *GUN1* regulatory sequences, we tagged the endogenous *GUN1* alleles (at the *GUN1* locus) through insertion of the mCherry and mCherry-AKI coding sequences in 3' of *GUN1* and *GUN1^{SG}* CDS by homologous recombination (Figure S7 and Mat. & Met.). Four tagged strains were obtained: *GUN1-mCherry, GUN1^{SG}-mCherry, GUN1-mCherry-AKI* and *GUN1^{SG}-mCherry-AKI*. Importantly, *GUN1-mCherry* and *GUN1-mCherry-AKI* tagged strains germinated like the wild-type while *GUN1^{SG}-mCHerry* and *GUN1^{SG}-mCHerry-AKI* tagged strains

bioRxiv preprint doi: https://doi.org/10.1101/2022.04.08.487612; this version posted April 10, 2022. The copyright holder for this preprint (which was not certified by peer review) is the author/funder, who has granted bioRxiv a license to display the preprint in perpetuity. It is made available under aCC-BY-NC-ND 4.0 International license.

germinated spontaneously on M2 medium like the *GUN1*^{SG} mutant. This suggested that the tagging by mCherry and mCherry-AKI did not modify GUN1 and GUN1^{SG} functions during ascospore germination. Each strain was crossed with strains expressing GFP markers tagging either mitochondria (mito-GFP) or peroxisomes (GFP-SKL) to obtain double tagged strains in the progeny (Ruprich-Robert et al., 2002; Sellem et al., 2007). Importantly, the presence of the *mito-GFP* or the *GFP-SKL* reporter genes did not modify ascospore germination. These double tagged strains allowed us to observe subcellular localization of GUN1 and GUN1^{SG} in mycelium (Figure 5) but not in melanized ascospores (Figure 6). For this purpose, each strain was crossed with the *PaPks1*^{136} mutant producing partially demelanized ascospores in order to obtain all the double tagged strains in *PaPks1*^{136} genetic background in the progeny. Contrary to the *PaPks1*^{193} mutation which leads to spontaneous ascospore germination (Figure 1B), the *PaPks1*^{136} mutation did not modify ascospore germination. All the *PaPks1*^{136} double tagged strains produced partially demelanized ascospores allowing fluorescence microscopic observations within ascospores and were isolated in both mating types (*mat*+ and *mat*-) in order to proceed to homozygous crosses for ascospore production and observation. Ascospores were observed either in M2 liquid medium (non-induction condition) or in G liquid medium for induction of ascospore germination (Figure 6). We observed in ascospores and in mycelium that GUN1-mCherry-AKI and GUN^{SG}-mCherry-AKI could co-localize with both mito-GFP and GFP-SKL, showing that both GUN1- and GUN1^{SG}-mCherry-AKI reporter proteins could be found in mitochondria and in peroxisomes (Figure 5). Careful comparison of GFP-tagging pattern and mCherry tagging pattern indicated that GUN1-mCherry-AKI and GUN^{SG}-mCherry-AKI could be absent in some mitochondria or in some peroxisomes. This was especially striking in "non-induction" condition (liquid M2) in *GUN1-mCherry-AKI mito-GFP* ascospores where no GUN1-mCherry-AKI co-localized with mitochondria (Figure 6). This data suggested that the distribution of GUN1-mCherry-AKI between mitochondria and peroxisomes might change upon germination induction, GUN1-mCherry-AKI localizing more frequently in mitochondria when ascospores germinate. In line with this, GUN1^{SG}-mCherry-AKI co-localization with mito-GFP was always important in mycelium and in ascospores, these latter germinating spontaneously in both M2 and G liquid medium.

We observed that GUN1-mCherry and GUN1^{SG}-mCherry co-localized only with the mito-GFP reporter in ascospores (Figure S8) as well as in mycelium (data not shown). This observation was consistent with previous studies on the localization of *G. zeae* CAT1-GFP (the ortholog of GUN1) showing that adding the GFP in C-terminus of the protein masked the PTS1 signal of CAT1 (Son et al., 2012). More generally, it has been shown that adding a tag after a C-terminal PTS1 signal abolishes import into peroxisomes, suggesting that GUN1-mCherry and GUN1^{SG}-mCherry could be mislocalized (Ast et al., 2013; Hooks et al., 2012). It is worth noting that ascospores in *GUN1-mCherry* tagged strain

bioRxiv preprint doi: https://doi.org/10.1101/2022.04.08.487612; this version posted April 10, 2022. The copyright holder for this preprint (which was not certified by peer review) is the author/funder, who has granted bioRxiv a license to display the preprint in perpetuity. It is made available under aCC-BY-NC-ND 4.0 International license.

germinated as wild-type and ascospores in *GUN1^{SG}-mCherry* tagged strain germinated spontaneously strongly suggesting that mislocalization of GUN1- or of GUN1^{SG}-mCherry did not affect ascospore germination. In contrast, whereas *GUN1-mCherry-AKI* and *GUN^{SG}-mCherry-AKI* strains grew as the wild-type on the different media tested, the *GUN1-mCherry* and *GUN^{SG}-mCherry* strains did not grow on oleic acid (Table S3). This result suggested that peroxisomal localization of GUN1 (and GUN1^{SG}) was required for oleic acid metabolism.

GUN1 acts upstream of the MAPK PaMpk2 pathway and of the PaNox2/PaPls1 complex

We have shown in previous studies that the MAPK *PaMpk2* pathway, *PaNox2*, its regulatory subunit *PaNoxR* and *PaPls1* are essential for ascospore germination in *P. anserina* : the deletion of these genes blocks ascospore germination (Brun et al., 2009; Lalucque et al., 2012; Lambou et al., 2008; Malagnac et al., 2004). We took advantage of the spontaneous germination phenotype of the *GUN1^{SG}* mutant to conduct epistasis studies in order to place *GUN1* in the regulatory cascade triggering ascospore germination. These studies were carried out by crossing *GUN1^{SG}* with the *ΔPaMpk2*, *ΔPaPls1* and *ΔPaNox2* strains. 48 homokaryotic spores were sown on M2 medium for each cross, but none of the germinated spores presented the *ΔPaMpk2*, *ΔPaPls1* or *ΔPaNox2* deletions (Table 4). This clearly showed that PaMpk2, PaPls1 and PaNox2 were required for germination in *GUN1^{SG}* ascospores and suggested that GUN1 acts upstream of PaMpk2, PaNox2 and PaPls1 in the cascade controlling ascospore germination. To confirm that GUN1 was upstream of the PaMpk2 MAPK pathway, we crossed the *ΔGUN1* strain with the Pa*MKK2^{c}* mutant carrying a constitutively active allele of *PaMKK2.* It has been previously shown that the *PaMKK2^{c}* mutation induces phosphorylation of PaMpk2 and spontaneous ascospore germination (Lalucque et al., 2012) (Figure 7). In the progeny of this cross, 40 homokaryotic ascospores were sown on M2 medium (Table 5). Every germinated ascospore carried *PaMKK2^{c}*, thus indicating that spontaneous germination on M2 medium was due to *PaMKK2^{c}*. Strikingly, *ΔGUN1 MKK2^{c}* ascospores (26/40) germinated on M2 medium, demonstrating that *MKK2^{c}*-induced ascospore germination was not blocked by the inactivation of *GUN1*. This confirmed that *GUN1* was upstream of the MAPK *PaMpk2* pathway in ascospore germination regulation. In line with this, we found that PaMpk2 was phosphorylated in *GUN1^{SG}* ascospores at a comparable level as in *PaMkk2^{c}* ascospores and as in wild-type ascospores induced for germination (Figure 7). Altogether, these data clearly indicated that *GUN1^{SG}* triggered spontaneous ascospore germination through the activation of the PaMpk2 MAPK pathway (Figure 8).

bioRxiv preprint doi: https://doi.org/10.1101/2022.04.08.487612; this version posted April 10, 2022. The copyright holder for this preprint (which was not certified by peer review) is the author/funder, who has granted bioRxiv a license to display the preprint in perpetuity. It is made available under aCC-BY-NC-ND 4.0 International license.

GUN1^{SG} induces spontaneous ascospore germination independently of *Pex7*

Peroxisomes are key organelles for germination. It has been shown that mutants of peroxisomal importomers such as *ΔPex5*, *ΔPex7* and *ΔPex13* produce partially demelanized ascospores impaired for germination (Peraza Reyes and Berteaux-Lecellier, 2013; Peraza-Reyes et al., 2011). We crossed *GUN1^{SG}* with the *ΔPex5 ΔPex7* double mutant and with the *ΔPex13* mutant and we checked whether *ΔPex5 GUN1^{SG}*, *ΔPex7 GUN1^{SG}* and *ΔPex13 GUN1^{SG}* double mutants could germinate when sown on G+YE germination medium (Table 6 & 7). None of the germinated ascospores carried *ΔPex5 or ΔPex13*, suggesting that *ΔPex5, ΔPex13, ΔPex5 GUN1^{SG}* and *ΔPex13 GUN1^{SG}* ascospores did not germinate. The fact that *ΔPex5* and *ΔPex13* were epistatic over *GUN1^{SG}* indicated that the function of both genes was required for *GUN1^{SG}*-induced ascospore germination. Very interestingly, 15 ascospores carrying *ΔPex7* germinated on G+YE germination medium. To test whether they also carried the *GUN1^{SG}* mutation, we analyzed spontaneous germination in the progeny of the mating tests performed to genotype spores (crossing with wild-type *S*). Abundant spontaneous germination was observed in bulk in this progeny showing that the 15 ascospores isolated were of the *ΔPex7 GUN1^{SG}* genotype and not *ΔPex7*. In other words, *GUN1^{SG}* suppressed the *ΔPex7* ascospore germination defect. This result indicated that germination was abolished in *ΔPex7* ascospores (as previously shown) and that *GUN1^{SG}* was epistatic over *ΔPex7*, inducing germination independently of *Pex7*.

Discussion

Despite its importance in the fungal life cycle, the regulation of ascospore germination in filamentous fungi has been poorly investigated so far. In this study, we aimed at uncovering new actors of this regulation pathway in *P. anserina*. To that end, we conducted a direct genetic screen, a particularly powerful approach to identify new genes. A majority of the mutants isolated, including all suppressors of *ΔPaNox2* and *ΔPaPls1*, showed spontaneous but abnormal ascospore germination. However, for six mutants, germination proceeded as in the wild-type through the germination pore at the tip of the ascospore. We hypothesized that in these mutants, ascospore dormancy was broken and that these were mutants specifically impaired in the control of ascospore germination. In this paper, we characterize the first of these six *Germination UNcontrolled-GUN* mutants, *GUN1^{SG}*. Although most of the spontaneous germination analyses were performed on M2 medium containing dextrin, the *GUN1^{SG}* mutant germinated on medium lacking carbon and nitrate sources indicating that in this mutant, control of dormancy escaped possible nutrient stimuli (data not shown). Through whole genome sequencing and genetic analyses, we showed that the gene mutated in *GUN1^{SG}* is the

bioRxiv preprint doi: https://doi.org/10.1101/2022.04.08.487612; this version posted April 10, 2022. The copyright holder for this preprint (which was not certified by peer review) is the author/funder, who has granted bioRxiv a license to display the preprint in perpetuity. It is made available under aCC-BY-NC-ND 4.0 International license.

Pa_6_1340 putative CDS. This CDS encodes a peroxisomal/mitochondrial Carnitine-acetyltransferase (CAT), a key metabolic enzyme involved in acetyl-CoA shuttling between peroxisomes and mitochondria (Elgersma et al., 1995; Strijbis and Distel, 2010). Gene expression of this CAT is significantly induced during ascospore germination, highlighting the pivotal role of this enzyme during this process (Demoor, unpublished data). The mutation in *GUN1*^{SG} CDS is a substitution of the conserved isoleucine 441 by an asparagin (I441N). 3-D modelisation of GUN1 and of mutated GUN1^{SG} proteins combined to *in silico* analyses of the stability of GUN1^{SG} predict a moderate effect of the I441N substitution on the overall stability of the protein but a deleterious effect on its activity. This prediction correlates with the recessive nature of the *GUN1*^{SG} mutation as well as the reduced CAT activity measured in *GUN1*^{SG}*,* both pointing to a loss-of-function of the *GUN1*^{SG} allele. Hence, GUN1 may act as an ascospore germination inhibitor. However, we also show that deletion of GUN1 leads to complete lack of germination and defect in melanin synthesis, indicating that GUN1 function is required for both processes and suggesting that the *GUN1*^{SG} allele is hypomorphic compared to *ΔGUN1* which is a null allele. Impairment of both germination and melanization are frequently observed in mutants of peroxisomal import machinery as well as in mutants of peroxisomal/mitochondrial β–oxidation (Boisnard et al., 2009; Peraza Reyes and Berteaux-Lecellier, 2013; Ruprich-Robert et al., 2002). Indeed, ascospores in the *ΔEchA* mutant impaired for mitochondrial β-oxidation and in the *ΔFox2* mutant impaired for peroxisomal β–oxidation, show reduced rate of germination. Interestingly, *ΔGUN1* exhibits complete lack of germination, suggesting that GUN1 and acetyl-CoA shuttling between peroxisomes and mitochondria is essential during activation of ascospore germination. As in many other fungi, we found a second CAT encoded in *P. anserina* genome. Deletion of this second CAT encoding gene, *Pa_3_7660/GUP1* (*GUN1 Paralog 1*), does not show any ascospore germination defect nor melanization defect, suggesting that this CAT has no role in both processes. Furthermore, while CAT activity in *ΔGUN1* and in *GUN1*^{SG} are reduced in mycelium, CAT activity in *ΔGUP1* resembles that of the wild-type, a situation similar to *M. oryzae*. In this plant pathogen, while the *GUN1* ortholog *Pth2* mutants show reduced CAT activity and reduced pathogenicity, the *ΔCrat2* K.O strain (*GUP1* ortholog) exhibits wild-type CAT activity and pathogenicity (Ramos-Pamplona and Naqvi, 2006).

As previously found in fungi (*M. oryzae*, *A. nidulans*, *G. zeae* and *S. cerevisiae*), we show that in *P. anserina,* the peroxisomal/mitochondrial CAT GUN1 is required for growth on acetate and oleic acid while the cytosolic CAT GUP1 is required for growth on acetate only, showing strong conservation of the function of both enzymes in fungal primary metabolism (Bhambra et al., 2006; Hynes et al., 2011; Liberti et al., 2013; Son et al., 2012; Swiegers et al., 2001). Nonetheless, GUN1 is required for growth on fatty acids, but we also show that oleic acid is toxic for *ΔGUN1* mutants, as previously demonstrated

bioRxiv preprint doi: https://doi.org/10.1101/2022.04.08.487612; this version posted April 10, 2022. The copyright holder for this preprint (which was not certified by peer review) is the author/funder, who has granted bioRxiv a license to display the preprint in perpetuity. It is made available under aCC-BY-NC-ND 4.0 International license.

for *Pex2*$^{-}$ mutants impaired for peroxisomal import (Ruprich-Robert et al., 2002). Indeed, both *ΔGUN1* and *ΔGUN1 ΔGUP1* strains grow better on Tween 40 control medium than on oleic acid medium containing similar amount of Tween 40. In contrast to peroxisomal import mutants such as *Pex2*$^{-}$, which are sterile in homozygous cross, fertility and ascospore production are only moderately decreased in *ΔGUN1* and *ΔGUN1 ΔGUP1.*

With the aim to understand how the mutation in *GUN1*^{SG} triggers breaking of dormancy, we explored both *GUN1*^{SG} CAT activity and *GUN1*^{SG} subcellular localization. *GUN1*^{SG} shows a similar loss of CAT activity in mycelium to that of *ΔGUN1*. However, *ΔGUN1* and *GUN1*^{SG} mutant strains exhibit noticeable phenotype discrepancies: *ΔGUN1* produces non-germinating demelanized ascospores while *GUN1*^{SG} produces spontaneously-germinating melanized ascospores and *GUN1*^{SG} grows as the wild-type on both oleic acid and acetate but not *ΔGUN1*. We were not able to measure CAT activity in ascospores and therefore to properly address the question of CAT activity during germination in *GUN1*^{SG} and *ΔGUN1.*

To explore how GUN1^{SG} causes spontaneous germination, both the wild-type GUN1 protein and the mutant GUN1^{SG} protein were tagged with mCherry or mCherry-AKI (AKI is the PTS1 peroxisomal import signal present in C-terminus of GUN1) and co-localization studies with GFP-tagged peroxisomes and GFP-tagged mitochondria were performed. Our data show that in mycelium as well as in ascospores, GUN1 is located both in peroxisomes and in mitochondria. This dual localization is in agreement i) with the predicted localization of this CAT bearing both a Mitochondrial Targeting Sequence (MTS) in N-terminus and the Peroxisomal Targeting Sequence (PTS1) AKI in C-terminus and ii) with studies of GUN1 orthologs in other fungi such as *A. nidulans* and *G. zeae* (Hynes et al., 2011; Son et al., 2012). In contrast, *M. oryzae* Pth2 was shown to only localize in peroxisomes (Bhambra et al., 2006). Attention must be drawn to the fact that there are no differences between GUN1 and GUN1^{SG} subcellular localization observed in mycelium as well as in ascospores subjected to germination induction: both proteins being more or less equally distributed between mitochondria and peroxisomes. Nevertheless, GUN1 seems to be almost exclusively located in peroxisomes in dormant ascospores not subjected to germination trigger. These data suggest that the breaking of dormancy in wild-type and in *GUN1*^{SG} ascospores may involve shuttling of GUN1^{SG} from peroxisomes to mitochondria. We show that, in keeping with the role of mitochondria in ascospore germination, the mislocalization of GUN1-mCherry (and GUN1^{SG}-mCherry) solely in mitochondria does not impair germination neither melanization of ascospores. However, *GUN1-mCherry* and *GUN1*^{SG}*-mCherry* strains do not grow on oleic acid, in the same way as *ΔGUN1*. A comparable effect has been reported in *A. nidulans* where mislocalized AcuJ in cytoplasm impairs growth on oleic acid but not on acetate (Hynes et al., 2011).

bioRxiv preprint doi: https://doi.org/10.1101/2022.04.08.487612; this version posted April 10, 2022. The copyright holder for this preprint (which was not certified by peer review) is the author/funder, who has granted bioRxiv a license to display the preprint in perpetuity. It is made available under aCC-BY-NC-ND 4.0 International license.

These data point to a central role of peroxisomal localization of GUN1 in oleic acid utilization independent of ascospore germination. However, it has been shown that peroxisomes are essential for germination in *P. anserina* and our data confirm that *ΔPex5* and *ΔPex13* strains lacking PTS1-dependent peroxisomal import machinery as well as *Δpex7* strains lacking PTS2-dependent peroxisomal import machinery cannot germinate (Peraza Reyes and Berteaux-Lecellier, 2013; Peraza-Reyes et al., 2011). How ascospores carrying mislocalized GUN1 germinate is an open question. Remarkably, we show that *GUN1*^{SG} can induce spontaneous ascospore germination independently of Pex7 and the PTS2-dependent peroxisomal import. Given that GUN1 bears a PTS1-AKI in C-terminus (and no internal PTS2) and that *ΔPex5* is epistatic over *GUN1*^{SG}, it is highly likely that GUN1 (and GUN1^{SG}) peroxisomal import is dependent on the PTS1 and not on the PTS2 import pathway.

Through the characterization of the *GUN* mutants, we aimed at uncovering new genes that control dormancy in ascospores. Genetic approaches in *P. anserina* and in particular the amenability to performing epistasis studies makes this model fungus a powerful system to decipher regulation pathways such as the one controlling ascospore germination. In this paper, we investigated the relationships between GUN1 and already known actors of ascospore germination: the *PaMpk2* MAPK pathway, the tetraspanin Pls1 and the NADPH oxidase Nox2 complex (Lalucque et al., 2012; Lambou et al., 2008; Malagnac et al., 2004). We show that GUN1^{SG} requires PaMpk2, PaNox2 and PaPls1 functions to induce spontaneous germination of ascospores. Conversely, the MAPKK constitutive *PaMKK2*^{c} allele inducing PaMpk2 phosphorylation and spontaneous ascospore germination does not require GUN1 function. Furthermore, we show that GUN1^{SG} controls the PaMpk2 pathway by activating PaMpk2 phosphorylation. Altogether, these data demonstrate that GUN1 acts upstream of the PaMpk2 pathway and the PaNox2/PaPls1 complex in the regulatory cascade controlling ascospore germination (Figure 8).

Melanin is a major component of appressorium cell wall in *M. oryzae* where it is involved in turgor pressure maintenance (Gómez and Nosanchuk, 2003). *M. oryzae* mutants such as *Pth2*$^{-}$ showing impairment of melanin synthesis cannot build up the turgor pressure necessary in the appressorium for host-penetration and are therefore non-pathogenic. As observed in the *PaPks1*^{193} mutant devoid of melanin biosynthesis, melanin in ascospores is important to avoid uncontrolled “accidental” germination (Coppin and Silar, 2007). The melanization defect exhibited by the *ΔGUN1* ascospores is likely due to lack of acetate supply to the dihydroxynaphthalene pathway involved in melanin biosynthesis, a defect shared by the *ΔechA* and *Δfox2 P. anserina* mutants, impaired in mitochondrial and in peroxisomal β-oxidation respectively (Boisnard et al., 2009; Coppin and Silar, 2007). But unlike *ΔechA* and *Δfox2* ascospores that germinate spontaneously, *ΔGUN1* ascospores do not, suggesting

bioRxiv preprint doi: https://doi.org/10.1101/2022.04.08.487612; this version posted April 10, 2022. The copyright holder for this preprint (which was not certified by peer review) is the author/funder, who has granted bioRxiv a license to display the preprint in perpetuity. It is made available under aCC-BY-NC-ND 4.0 International license.

that the melanization defect in *ΔGUN1* ascospores is not sufficient to induce spontaneous germination. Accordingly, Tricyclazole, a fungicide inhibiting melanin biosynthesis or the *PaPks1*^{193} mutation blocking melanin production (Coppin and Silar, 2007), suppress the germination defect of *ΔGUN1* ascospores. Indeed, *PaPks1*^{193} *ΔGUN1* ascospores germinate spontaneously (data not shown). Hence, it is likely that in *ΔGUN1* ascospores, residual melanin in cell wall is enough to avoid "accidental" spontaneous germination.

The fact that Tricyclazole and *PaPks*^{193} null mutation trigger germination of *ΔGUN1* ascospores suggests that these ascospores are competent for formation of the germination peg and eventually hyphal growth but that they might be blocked in the formation of the germination pore. The formation of a pore in melanized ascopores is a process sharing similarities with the formation of the pore in *M. oryzae* appressorium (Malagnac et al., 2008). In this pathogenic fungus, the formation of the appressorial pore is preceded by the formation of a septin ring required for actin cytoskeleton remodeling and appressorial pore solidity. In-depth studies in *M. oryzae* have deciphered the intricate genetic signaling, culminating in the setting up of this septin ring (Dagdas et al., 2012; Ryder et al., 2019). Among other regulatory components the Fus3/Pmk1/PaMpk2 pathway and the NoxB/Pls1 complex play a key role in septin ring assembly. The fact that both pathways are also essential for ascospore germination in *P. anserina*, *N. crassa* and *S. macrospora*, three species producing melanized ascospores lead us to hypothesize that a similar process involving septin ring assembly and cytoskeleton remodeling may take place to initiate the formation of the germination pore. Given the similarities in the regulation of appressorium functioning and ascospore germination when those are melanized, we speculate that studying and discovering new genes controlling ascospore germination in *P. anserina* may lead to the discovery of new pathogenesis factors controlling appressorium development in pathogenic fungi. The characterization of *GUN1*, the ortholog of *M. oryzae Pth2* represents a proof of concept. The characterization of the other *GUN* mutants and in the future, the isolation of new *GUN* mutants will be of great interest to better understand ascospore germination but also to discover new pathogenic factors, killing two birds with the same stone.

Materials and Methods

Strains and culture conditions

The strains used in this study are all listed in Table 1. All of these *P. anserina* strains derive from the wild-type *S* strain, ensuring a homogenous genetic background (Espagne et al., 2008; Rizet, 1952). The *PaPks1*^{193} mutant for the polyketide synthase encoding gene acting at the first step of melanin

bioRxiv preprint doi: https://doi.org/10.1101/2022.04.08.487612; this version posted April 10, 2022. The copyright holder for this preprint (which was not certified by peer review) is the author/funder, who has granted bioRxiv a license to display the preprint in perpetuity. It is made available under aCC-BY-NC-ND 4.0 International license.

synthesis is described in (Coppin and Silar, 2007). Standard culture conditions, media and genetic methods for *P. anserina* were described in (Rizet and Engelmann, 1949) and can be found in (Silar, 2020) and on the *Podospora* data base http://podospora.i2bc.paris-saclay.fr/. The composition of the M0 and M3 media is similar to that of the M2 medium, except that dextrin is replaced by glucose in the M3 medium (5,5 $g.L^{-1}$), while no carbon source is added in the M0 medium. This M0 medium was used as a basis for the development of media in which the only carbon source was sodium acetate (60 mM) or oleic acid (Sigma-Aldrich) (6 mM) dissolved in Tween 40 (0.5 %). A control medium M0 with only Tween 40 (0.5%) was also used. The germination medium used in this study was supplemented with Yeast extract (G+YE) 5 $g.L^{-1}$. In order to allow germination in strains producing ascospores unable to germinate, crosses were set up on M2 medium supplemented with Tricyclazole (1 $\mu g.mL^{-1}$), a fungicide impairing melanin synthesis in *P. anserina* ascospores (Coppin and Silar, 2007).

Genetic screening of constitutively germinating mutants

It has been shown that wild-type *P. anserina* ascospores do not germinate on standard M2 medium and that the *ΔPaNox2* and *ΔPls1* mutant strains produce ascospores unable to germinate on all tested media (Lambou et al., 2008; Malagnac et al., 2004). With the aim to isolate mutants producing spontaneously germinating ascospores, a UV mutagenesis was performed on auto-fertile *mat-/mat+*, wild-type *S*, *ΔPaNox2* and *ΔPls1* strains. The selection process of the germination mutants is summarized in Figure S1. Shortly after UV exposure, followed by a one-day culture in the dark to prevent repair by photoreactivation, the mutated strains were grown on standard M2 medium for one week until they developed mature ascospores-producing perithecia. In order to recover spontaneously germinating ascospores, M2 medium plates were put on top of the plates bearing perithecia, which allowed ascospores to be harvested in bulk on M2 medium. In *P. anserina*, most of the progeny is composed of heterokaryotic *mat+/mat-* ascospores leading to self-fertile mycelium upon germination (Silar, 2013). The thalli produced by the spontaneously-germinating ascospores were incubated until they formed mature perithecia projecting their ascospores. Ascospores produced by these perithecia were individually collected with a needle and transplanted onto M2 medium. To ensure their independence, a single mutant (*i.e.*, a single spontaneously-germinating homokaryotic ascospore) per initial plate was selected for further analyses. For every mutant, progeny analysis of mutant X wild-type *S* crosses showed that a single mutated locus was responsible for the mutant phenotype (*i.e.,* spontaneous germination of ascospores). For mutants recovered with the *ΔPaNox2* and *ΔPls1* strains, genetic analyses showed that the mutations enabling germination were unlinked to the *ΔPaNox2* and *ΔPls1* mutations, respectively. Homokaryotic *mat-* and *mat+* mutant

bioRxiv preprint doi: https://doi.org/10.1101/2022.04.08.487612; this version posted April 10, 2022. The copyright holder for this preprint (which was not certified by peer review) is the author/funder, who has granted bioRxiv a license to display the preprint in perpetuity. It is made available under aCC-BY-NC-ND 4.0 International license.

strains were isolated from the progenies and homozygous mutant crosses were performed to check for the fertility/sterility of the mutants. For every isolated strain, microscopic observations were also performed to determine whether the ascospores germinated through the germination pore at the tip of the ascospore or through any other part of the ascospore (data not shown).

Tetrad analysis in the *GUN1^{SG}* and in the *ΔGUN1* strains

Demonstration of the recessivity of the *GUN1^{SG}* allele: *P. anserina* produces mainly asci containing four heterokaryotic/dikaryotic ascospores, allowing non-ordered tetrad analysis of first division segregation (FDS) asci and second division segregation (SDS) asci. To determine dominance/recessivity of the *GUN1^{SG}* allele, we crossed the *GUN1^{SG}* mutant with the *WT*. In thirty asci of the progeny, we found that 16 asci contained four heterokaryotic ascospores unable to germinate on M2 medium (4 [non-germinating] ascospores) and 14 asci contained different number of ascospores germinating spontaneously: 3 [non-germinating]; 1 [germinating] or 2 [non-germinating]; 2 [germinating] ascospores. Importantly, we never observed asci containing more than 2 ascospores germinating on M2 medium. Assuming some ascospore germination failure due to their manipulation, especially the ones germinating spontaneously, we concluded that i) asci of the first type were SDS asci containing 4 *GUN1^{SG}/GUN1* ascospores of the [WT] phenotype (non-germinating on M2 medium), ii) asci of the second type were FDS asci containing 2 *GUN1^{SG} /GUN1^{SG}* of the [GUN] Germination UNcontrolled phenotype (germinating on M2 medium) and 2 *GUN1/GUN1* ascospores of the [WT] phenotype. The *GUN1^{SG}* allele was thus recessive against the wild-type *GUN1* allele (*i.e.,* only *GUN1^{SG}/GUN1^{SG}* ascospores germinated on M2 medium but not the *GUN1^{SG}/GUN1* ones).

Demonstration of the recessivity of the *ΔPa_6_1340::hygR* (*ΔGUN1*) allele: The recessivity of the *ΔPa_6_1340::hygR* (*ΔGUN1*) phenotypes was tested by crossing *ΔPa_6_1340::hygR* with the wild-type. We sowed 20 asci on G+YE germination medium and we obtained i) 9 asci containing 2 [demelanized, non-germinating] and 2 [melanized, germinating, hygS] ascospores; these were identified as First Division Segregation (FDS) asci containing 2 *ΔPa_6_1340::hygR*/*ΔPa_6_1340::hygR* and 2 wild-type *Pa_6_1340*/*Pa_6_1340* ascospores respectively. The 11 other asci contained 4 [melanized, germinating, hygR] ascospores which were identified as SDS asci composed of 4 *ΔPa_6_1340::hygR*/*Pa_6_1340* ascospores. These data demonstrated that the phenotypes due to *ΔPa_6_1340::hygR* deletion were recessive and that SDS rate for the *Pa_6_1340* locus was 55 %.

bioRxiv preprint doi: https://doi.org/10.1101/2022.04.08.487612; this version posted April 10, 2022. The copyright holder for this preprint (which was not certified by peer review) is the author/funder, who has granted bioRxiv a license to display the preprint in perpetuity. It is made available under aCC-BY-NC-ND 4.0 International license.

Complementation test between the *ΔPa_6_1340::hygR* (*ΔGUN1*) and the *GUN1^{SG}* alleles: We crossed *GUN1^{SG}* with *ΔPa_6_1340::hygR* and we reasoned that if *ΔPa_6_1340::hygR* and *GUN1^{SG}* are allelic, no functional complementation in heterokaryotic ascospores in SDS asci is expected for the spontaneous germination of *GUN1^{SG}*: *ΔPa_6_1340::hygR/GUN1^{SG}* ascospores germinate spontaneously on M2 medium; in contrast, if *GUN1^{SG}* and *ΔPa_6_1340::hygR* are not allelic, functional complementation leading to restoration of wild-type phenotype is expected: *Pa_6_1340::hygR/Pa_6_1340 GUN1^{SG}/GUN1* heterokaryotic ascospores in SDS asci germinate only on G+YE medium but not on M2 medium. The SDS asci (54%) (n=50) were easily recognized since they contained 4 [hygR, melanized] ascospores, compared to the FDS asci, containing 2 [hygS, melanized] ascospores and 2 [non germinating, demelanized] ascospores. Strikingly, we observed that heterokaryotic ascospores in SDS asci germinated spontaneously on M2 medium showing that *GUN1^{SG}* and *ΔPa_6_1340* were allelic. This demonstrated that *Pa_6_1340* was the gene mutated in the *GUN1^{SG}* mutant responsible for the spontaneous germination phenotype.

GUN1^{SG} genome sequencing and analysis

In a first step towards identifying the gene mutated in *GUN1^{SG}* through whole genome sequencing, we backcrossed the mutant for five generations with the parental wild-type *S* strain as to eliminate any mutation unrelated to the mutant phenotype. The *GUN1^{SG}* genomic DNA was then extracted as described in (Lecellier and Silar, 1994). The genomic DNA was then subjected to complete sequencing with the Illumina technology at the Imagif facility, Gif-sur-Yvette (CNRS, I2BC Sequencing Facility, https://www.i2bc.paris-saclay.fr/spip.php?article1184&lang=en). Custom-made libraries had 300 bp inserts and sequencing was 76-bp paired-end. Coverage was 80-fold. The sequence reads were then mapped onto the latest version of the reference genome of the *S* strain (Grognet et al., 2014). Potential mutations were detected using Samtools and bcftools on the Galaxy web server (https://usegalaxy.org/).

Deletion of *GUN1*, *GUP1* and construction of the double *ΔGUN1 ΔGUP1* strain

***ΔGUN1*:** the deletion of *Pa_6_1340/GUN1* and its paralog *Pa_3_7660/GUP1* were performed using deletion cassettes made of two overlapping PCR fragments (Figure S3 & S5) (Lalucque et al., 2012). This method is based on the generation of two DNA PCR fragments carrying a resistance marker flanked by either 5′ or 3′ flanking sequences of the targeted gene. For *Pa_6_1340/GUN1*, we first amplified the 803 bp-long 5′ and 486 bp-long 3′ flanking regions of the *S* strain DNA by PCR with

bioRxiv preprint doi: https://doi.org/10.1101/2022.04.08.487612; this version posted April 10, 2022. The copyright holder for this preprint (which was not certified by peer review) is the author/funder, who has granted bioRxiv a license to display the preprint in perpetuity. It is made available under aCC-BY-NC-ND 4.0 International license.

primers pairs: 1340_1/1340_2 and 1340_3/1340_4 respectively (Table S2). At the same time, the hygromycin B resistance marker was amplified with 1340_MkF and 1340_MkR (Table S2) from the pBC-hygR vector (Silar, 1995). In a second PCR round, using primers 1340_1 and 1340-MkR, and 1340-MkF and 1340_4, the resistance marker was fused with the 5' and with the 3' flanking regions respectively. Both PCR products were used to transform a *Δmus51*::*genR* strain, in which the *mus51* gene involved in the NHEJ repair system is replaced by a geneticin resistance gene [genR], allowing high rate of homologous recombination (El-Khoury et al., 2008). Two hygromycin B-resistant [hygR] transformants were obtained. Each one was crossed with the wild-type *S* strain. We observed in the progeny that homokaryotic [hygR] ascospores did not germinate. Consequently, crosses were performed on M2 medium supplemented with Tricyclazole, leading to spontaneous germination of ascospores (Coppin and Silar, 2007). The [hygR] thalli coming from spontaneously germinating ascospores were selected on M2 medium supplemented with hygromycin B, fragmented and [hygR, phleoS] *ΔGUN1::hygR* homokaryotic mycelia of each mating type were isolated. Deletion of *Pa_6_1340* was verified by Southern blot analysis (Figure S3). Only one strain was selected for further analyses.

***ΔGUP1*:** the same protocol was performed to produce the deletion cassettes for *Pa_3_7660/GUP1*. Using the primers pairs: 7660_F1/7660_R2 and 7660_R3/7660_R4 (Table S2), the 1104 bp-long 5' and 1011 bp-long 3' *Pa_3_7660* flanking regions were PCR-amplified, while the phleomycin resistance marker was amplified with primers 7660_MkF and 7660_MkR (Table S2) from a pBC-phleoR plasmid (Silar, 1995). In a second PCR round, using primers 7660_F1 and 7660_MkR, and 7660_MkF and 7660_R4 the resistance marker was fused with the 5' and the 3' flanking regions. Both PCR products were used to transform a *Δmus51::genR* strain. 26 phleomycin-resistant [phleoR] transformants were obtained and two independent [phleoR, genS] *ΔGUP1::phleoR* strains were selected from the progeny of a cross with the wild-type *S* strain (germination of *ΔGUP1::phleoR* ascospores was as wild-type). Deletion in these two independent strains was verified by Southern blot analysis (Figure S5). Only one strain was selected for further analyses.

ΔGUN1 ΔGUP1: with the aim to construct the *ΔGUN1 ΔGUP1* double mutant, we crossed *ΔGUN1* with *ΔGUP1* on M2 supplemented with Tricyclazole, we selected [hygR, phleoR] mycelia from spontaneously germinating ascospores on M2 medium supplemented with hygromycin and phleomycin. These mycelia were fragmented and homokaryotic [hygR, phleoR] *ΔGUN1 ΔGUP1* strain of each mating type was isolated.

bioRxiv preprint doi: https://doi.org/10.1101/2022.04.08.487612; this version posted April 10, 2022. The copyright holder for this preprint (which was not certified by peer review) is the author/funder, who has granted bioRxiv a license to display the preprint in perpetuity. It is made available under aCC-BY-NC-ND 4.0 International license.

Plasmid constructions for the complementation of *GUN1^{SG}*, *ΔGUN1* and *ΔGUP1*

Construction of pGUN1: The *Pa_6_1340/GUN1* CDS, its 803 bp 5' upstream and 486 bp 3' downstream sequences were amplified by PCR from wild-type *S* genomic DNA using 1340_1 and 1340_4 primers (Table S2). The PCR product obtained was cloned blunt-end into pBC-genR plasmid carrying a geneticin resistance marker digested by *E*coRV to produce the pBC-GUN1-genR plasmid (renamed pGUN1 for sake of simplicity). The insert was verified by sequencing (data not shown). This plasmid was used to transform the *ΔGUN1::hygR* deletion strain. 2 [genR] transformants were obtained and checked for the restoration of wild-type phenotypes in ascospores. To that end, two of these transformants were crossed with the *ΔGUN1::hygR* strain. In the progeny of both crosses, [hygR, genR] melanized homokaryotic ascospores germinated (on G+YE germination medium) allowing us to purify *ΔGUN1 pGUN1 mat*+ and *mat*- homokaryotic strains and to show that wild-type *GUN1* complemented the *ΔGUN1* mutation. [hygS, genR] *GUN1 pGUN1* homokaryotic ascospores were also isolated in the progeny. These ascospores germinated as the wild-type. The pGUN1 was also used to transform the *GUN1^{SG}* mutant. 3 [genR] transformants were obtained and crossed with *GUN1^{SG}* to assess restoration of wild-type germination in the progeny. For one transformant, we observed that *GUN1^{SG} pGUN1* progeny showed wild-type ascospore germination, *i.e GUN1^{SG} pGUN1* spores did not germinate spontaneously on M2 medium but germinated on G+YE germination medium, showing that ectopic wild-type *GUN1* complemented the *GUN1^{SG}* mutant (Table 3).

Construction of pGUP1: the *Pa_3_7660/GUP1* CDS, its 1104 bp 5'upstream and 1011 bp 3' dowstream sequences were amplified by PCR from wild-type *S* genomic DNA using primers 7660_F1 and 7660_R4 (Table S2). The PCR product obtained was cloned blunt-end into pBC-nouR (carrying a nourseothricin resistance marker) digested by *E*coRV to produce the *pBC-GUP1-nouR* plasmid (renamed pGUP1). The pGUP1 plasmid was used to transform the *ΔGUP1::phleoR* deletion strain. 17 [nouR] transformants were obtained and checked for the restoration of growth on acetate [ace +]. 14 of them were [ace +], showing that wild-type *GUP1* complemented *ΔGUP1* mutation. Two of these complemented transformants were crossed with the wild-type *S* strain and [phleoR, nouR] *ΔGUP1 pGUP1* as well as [phleoS, nouR] *ΔGUP1 pGUP1* homokaryotic *mat*+ and *mat*- strains were purified.

Plasmid construction for GUN1- and GUN1^{SG}-mCherry/mCherry-AKI tagging

Two kinds of tagging were undertaken: one with the mCherry-AKI reporter protein, carrying the AKI PTS1 peroxisome targeting signal present in C-terminus of GUN1, added in C-terminus of the mCherry,

bioRxiv preprint doi: https://doi.org/10.1101/2022.04.08.487612; this version posted April 10, 2022. The copyright holder for this preprint (which was not certified by peer review) is the author/funder, who has granted bioRxiv a license to display the preprint in perpetuity. It is made available under aCC-BY-NC-ND 4.0 International license.

and the second with the standard mCherry without the AKI PTS1 signal. To this end, we constructed plasmids allowing integration of the *mCherry-AKI* CDS or the *mCherry* CDS in 3' (and in frame) of *GUN1* or of *GUN1^{SG}* CDS at the endogenous *GUN1* locus by homologous recombination (Figure S7). To achieve this, the 621 bp region upstream of the stop codon (but downstream of the mutation present in the *GUN1^{SG}* allele) was PCR-amplified with primers 1340GFP_F2 and 1340GFP_R1 (Table S2) designed to incorporate the *Apa*I and *Xho*I restriction sites in the sequence respectively. The PCR product was cloned blunt-end into the pBC-genR plasmid previously digested with *E*coRV. The insert was then sequenced, digested with the restriction enzymes *Apa*I and *Xho*I and gel purified to be finally cloned upstream to the mCherry CDS into the pBC-mCherry-hygR plasmid digested by *Apa*I and *Xho*I (Table S2). This pBC-GUN1-mCherry-hygR (renamed pGUN1-mCherry for sake of simplicity) plasmid was sequenced and transformed into both *Δmus52::genR* and *GUN1^{SG} Δmus52::genR* and [hygR] transformants were selected. We obtained 1 [hygR] transformant for *Δmus52::genR* and 2 [hygR] transformants for *GUN1^{SG} Δmus52::genR*. Every transformant showed red fluorescence under the microscope. Correct *GUN1-mCherry* and *GUN1^{SG}-mCherry* gene fusions were verified by sequencing (data not shown). One transformant of each genotype was selected and crossed with the *S* strain to purify [hygR, genS] *GUN1-mCherry* and *GUN1^{SG}-mCherry* homokaryotic *mat*- and *mat*+ strains in the progeny. Finally, we observed that *GUN1-mCherry* ascospores germinated as the wild-type and that *GUN1^{SG}-mCherry* ascospores germinated spontaneously on M2 medium. To construct the pBC-GUN1-mCherry-AKI-nouR plasmid, we amplified by PCR the insert present in pGUN1-mCherry with primers 1340GFP_F2 and mCH_AKIR1, the latter primer allowing addition of the AKI coding sequence at the end of the mCHerrry (Figure S7). This 1341 bp PCR fragment was cloned blunt-end into pBC-nouR digested with *E*coRV to give the pBC-GUN1-mCherry-AKI-nouR plasmid (renamed pGUN1-mCherry-AKI). The construction was sequenced and transformed into the *Δmus52::genR* strain. We selected one [nouR] transformant showing red fluorescence under the microscope and we crossed it with the wild-type *S* strain to purify [genS, nouR] *GUN1-mCHerry-AKI mat*+ and *mat*- strains. This *GUN1-mCHerry-AKI* strain showed red fluorescence under the microscope and correct GUN1-mCHerry-AKI gene fusion was verified by sequencing (data not shown). This *GUN1-mCherry-AKI* strain was then crossed with the *GUN1^{SG}* mutant to generate the *GUN1^{SG}-mCherry-AKI* strain by meiotic recombination between the *GUN1^{SG}* mutation and the mCherry-AKI-nouR insertion. In the progeny of this cross, we isolated 13 thalli from spontaneously germinating [nouR] ascospores on M2 medium supplemented with Nourseothricin. All these isolates were heterokaryotic auto-fertile (*mat+ / mat-*). Since the *GUN1^{SG}* mutation is recessive, we hypothesized that these isolates arose from *GUN1^{SG}-mCherry-AKI/GUN1^{SG}-mCherry-AKI* recombinated heterokaryotic ascospores. One of these isolates was fragmented and [NouR] homokaryotic *GUN1^{SG}-mCherry-AKI* ascospores of each mating type were

bioRxiv preprint doi: https://doi.org/10.1101/2022.04.08.487612; this version posted April 10, 2022. The copyright holder for this preprint (which was not certified by peer review) is the author/funder, who has granted bioRxiv a license to display the preprint in perpetuity. It is made available under aCC-BY-NC-ND 4.0 International license.

purified establishing the *GUN1^{SG}-mCherry-AKI* strain. Red fluorescence in this final strain was verified and the presence of the *GUN1^{SG}* mutation as well as correct *mCherry-AKI* integration were verified by sequencing (data not shown). Germination of *GUN1^{SG}-mCherry-AKI* ascospores was spontaneous on M2 medium as for the *GUN1^{SG}* mutant.

Mycelium fragmentation and strain purification

For strains carrying the *ΔGUN1* deletion and which therefore cannot germinate, homozygous crosses were performed on M2 medium supplemented with Tricyclazole (1 µg.mL^{-1}), leading to spontaneous germination of ascospores. The purification of homokaryotic strains was performed through mycelium fragmentation as follows: a small implant of the thallus of interest (0.5 cm²) was set in 2 mL tube containing 500 µL H_2O and ground using a FastPrep (TeSeE - Biorad, Hercules, California, United States) (20s, 5000 rpm). 100 µL of the fragmented mycelium were then spread on an agar plate, and small hyphal fragments were isolated, using a binocular (magnification x40). These isolates were then placed on M2 medium and cultured for 2 days at 27°C. Homokaryotic (*mat+* or *mat-*) versus auto-fertile heterokaryotic (*mat+*/*mat-*) genotype of isolates was determined through a mat-type test using wild-type *S mat+* and *mat-* strains.

Fertility assay

Fertility was assayed by generating auto-fertile *mat+/mat–* heterokaryons of the tested strains. To this end, implants (0.5 cm²) of each mating type of the strains of interest were placed in 2 mL tubes containing 500 µL H_2O and ground using a FastPrep (TeSeE - Biorad, Hercules, California, United States) (20s, 5000 rpm). 10 µL of each heterokaryon were dropped onto M2 medium and cultured for 10 days at 27 °C with light. A qualitative evaluation of perithecia formation directly on the plates and of ascospore production projected on the Petri plate lids during 4 days was performed. Every heterokaryon were analyzed in duplicate.

Cellophane penetration assay

An implant of each tested strain was placed on a cellophane layer (Biorad, Hercules, California, United States). After 2-, 3-, 4-, and 5-days growth at 27°C, the cellophane layer was removed, and the presence of mycelium in the medium checked with a binocular to determine if the strain had breached

bioRxiv preprint doi: https://doi.org/10.1101/2022.04.08.487612; this version posted April 10, 2022. The copyright holder for this preprint (which was not certified by peer review) is the author/funder, who has granted bioRxiv a license to display the preprint in perpetuity. It is made available under aCC-BY-NC-ND 4.0 International license.

the cellophane layer. In parallele, the presence/absence and the morphology of appressoria in the cellophane layer were observed under the microscope as described in (Brun et al., 2009; Demoor et al., 2019).

Microscopic observations

Ascospores observations were performed in Ibidi 8-wells chamber micro-slides (Gräfelfing, Germany). Each well was filled with 200 µL of either M2 or modified G liquid medium: the quantity of Bacto peptone was divided by two compared to standard G medium in order to reduce the fluorescing background noise due to Bacto peptone. Germination induction of this modified medium was not altered (data not shown). Crosses were performed on standard M2 medium. Once perithecia were mature, agar plugs bearing the perithecia were cut and placed above the microscopic chambers upside-down. Perithecia were left to project their ascospores into the well for 5 hours. For mycelium observations, small squares of medium (1 cm^2) with grown mycelium on it were cut at the edge of the thallus and placed upside-down in water on a coverslip of a microscopic chamber. Images were taken with an inverted microscope Zeiss spinning disk CSU-X1 (Oberkochen, Germany), with 4 lasers (405nm, 488nm, 561nm, 640nm) for fluorescence observations and their associated filters and a sCMOS PRIME95 (Photometrics) camera at the Imagoseine Imaging Facility: https://imagoseine.ijm.fr/676/accueil.htm. The images were analysed with Fiji (Schindelin et al., 2012).

Phylogenetic analysis

Fungal genes homologous to *GUN1* were searched by BLAST in GenBanK and Mycocosm (Benson et al., 2013; Grigoriev et al., 2014), using the default parameters with the GUN1 protein sequence as query. For a selection of *Ascomycota*, *Basidiomycota* and *Mucoromycota* species, hits with an e-value lower than 10^{-5} were selected. Research for other homologs was carried out for each selected species on OrthoDB (Kriventseva et al., 2019). The alignment was performed with MAFFT (Katoh et al., 2005) and manually refined using Jalview (Waterhouse et al., 2009). The phylogenetic tree was built using the maximum likelihood method (PhyML software using the default parameters) (Guindon and Gascuel, 2003). The tree was visualized on the iTOL server (Letunic and Bork, 2007). Bootstrap values are expressed as percentages of 100 replicates (Figure S4). The GUN1 I441 residue conservation was assessed by visualizing the alignment on Jalview (Figure S6) (Waterhouse et al., 2009).

bioRxiv preprint doi: https://doi.org/10.1101/2022.04.08.487612; this version posted April 10, 2022. The copyright holder for this preprint (which was not certified by peer review) is the author/funder, who has granted bioRxiv a license to display the preprint in perpetuity. It is made available under aCC-BY-NC-ND 4.0 International license.

Bioinformatic analysis of the GUN1 protein

The analysis of the GUN1 protein sequence was carried out using multiple tools: CD-search: https://www.ncbi.nlm.nih.gov/Structure/cdd/wrpsb.cgi (Marchler-Bauer and Bryant, 2004), Interproscan: https://www.ebi.ac.uk/interpro/search/sequence/ (Quevillon et al., 2005) and Prosite: https://prosite.expasy.org/ (Sigrist et al., 2010). Prediction of its localization was realized using wolfPSORT: https://wolfpsort.hgc.jp/ (Horton et al., 2007). For research of a Mitochondrial Targeting Signal (MTS), we also used MitoFates: http://mitf.cbrc.jp/MitoFates/cgi-bin/top.cgi (Fukasawa et al., 2015). 3D homology modelling was performed using Swiss model: https://swissmodel.expasy.org/ (Waterhouse et al., 2018), and a 3D structure prediction of the GUN1 protein was achieved using the I-TASSER platform available at: https://zhanglab.ccmb.med.umich.edu/I-TASSER/ (Roy et al., 2010). The predicted effect of the missense I447N mutation in *GUN1*^{SG} on protein structure and stability was assessed using the STRUM server (https://zhanglab.ccmb.med.umich.edu/STRUM/) and the PROVEAN online tool (http://provean.jcvi.org/index.php) respectively (Choi and Chan, 2015; Quan et al., 2016).

CAT activity assay

Mycelium proteins extraction: Mycelia growing on M2 medium (2 confluent plates per strain) were harvested after 2 days, and placed in 2 mL tubes each one containing a tungsten bead (diameter 3 mm), 1 mL of potassium phosphate buffer (pH=7.4) supplemented with EDTA 2 mM and ground in a TissueLyser II apparatus (Qiagene, Hilden, Germany) at 30rpm/s for 4 min at 4°C. The lysate was centrifugated at 4°C for 20 min at 17000 g and the supernatant was separated from the pellet (cell debris). The protein concentration in the supernatant was measured by the spectrophotometric Bradford method (Sigma Chemical Co., St Louis). **Ascospore proteins extraction**: each strain was crossed (in homozygous crossing) on at least 5 M2 medium plates. When perithecia were mature, the projected ascospores were collected on agar plates topped with a cellophane layer and pulled together in a 2 mL tube for each strain, each one containing a tungsten bead (diameter 3 mm). Immediately after harvesting, each tube was flash frozen in liquid nitrogen. Ascospores were dry-crushed in a TissueLyser II apparatus (Qiagene, Hilden, Germany) at 30 rpm/s for 4 min at -80°C. Ascospores were maintained at -80°C in precooled TissueLyser blocks. The crushed ascospores were resuspended in 200 µL of potassium phosphate buffer (pH=7.4) supplemented with EDTA 2 mM. The lysate was centrifugated at 4°C for 20 min at 17000 g and the supernatant was separated from the

bioRxiv preprint doi: https://doi.org/10.1101/2022.04.08.487612; this version posted April 10, 2022. The copyright holder for this preprint (which was not certified by peer review) is the author/funder, who has granted bioRxiv a license to display the preprint in perpetuity. It is made available under aCC-BY-NC-ND 4.0 International license.

pellet (cell debris). The protein concentration in the supernatant was estimated by the spectrophotometric Bradford method (Sigma Chemical Co., St Louis). **Carnitine-acetyltransferase assay:** Carnitine-acetyltransferase (CAT) activity was assayed as described in (Kawamoto et al., 1978). The reaction was monitored spectrophotometrically at room temperature by following the release of CoA-SH from acetyl-CoA using the thiol reagent 5, 5'-dithiobis-nitrobenzoic acid (DTNB-Sigma Chemical Co., St Louis). The reaction mixture contained 100 mM Tris-HCl buffer (pH 7.8) 0.05 mM acetyl-CoA (Sigma Chemical Co., St Louis), 0.1 mM DTNB, 22 mM DL-carnitine chloride (Sigma Chemical Co., St Louis) and protein extract in final volume I.0 mL. The reaction was initiated by adding a volume of the protein extract and the increase in absorbance was followed at 412 nm. CAT activities were determined by measuring initial velocity of the CoA-SH production reaction, and then reported as the activity ratio of the wild-type *S* strain. Standard deviations and statistical analyses were calculated on 4 to 7 biological replicates. Eventually, CAT activities were compared using a Fisher-Pitman Permutation Test.

Western Blot analysis

PaMpk2 phosphorylation was assessed as described in (Lalucque et al., 2012). Ascospores produced by homozygous crosses of the *S* strain, the *PaMKK2*^{c} mutant and the *GUN1*^{5G} mutant were harvested on agar plates topped with a cellophane layer to facilitate the ascospores harvesting process. For germination induction, a cellophane layer with wild-type ascospores was transferred on G+YE medium for 2 hours. Once collected, ascospores were flash frozen in liquid nitrogen, then dry-disrupted in a Micro-Dismembrator (Sartorius) at 2600 rpm for 1 min at -80°C. Crushed ascospores were resuspended in Laemli buffer, placed 5 minutes at 100 °C, then centrifuged for 15 min at 14000 rpm. Samples were placed on a 15% SDS-PAGE gel 1 mm thick, and migrated for 3 h at 130V, 25mA/gel and 25W. The gel was then transferred onto a PVDF membrane. Hybridization with the anti p44/p42, or anti-phospho p44/42 (Cell Signaling Technology) antibodies, diluted to 1/1000, was carried out overnight at 4°C. Hybridization with the second antibody coupled to peroxidase (GEHealthcare), diluted to 1/1000, was carried out for 1 h at room temperature. For the revelation, the Immobilion® chemiluminescence kit (Millipore) was used according to the supplier's recommendations.

Acknowledgments

We want to thank the ImagoSeine facility, member of the France BioImaging infrastructure supported by the French National Research Agency (ANR-10-INSB-04, « Investmentsfit the future »). We also

bioRxiv preprint doi: https://doi.org/10.1101/2022.04.08.487612; this version posted April 10, 2022. The copyright holder for this preprint (which was not certified by peer review) is the author/funder, who has granted bioRxiv a license to display the preprint in perpetuity. It is made available under aCC-BY-NC-ND 4.0 International license.

thank Sylvie Cangemi for her precious help in preparing the various media used in this study and Elizabeth Guinot Bordini for English proofreading.

Authors contribution

AD: experimentation and manuscript writing; IL: experimentation; RF: experimentation; CL: statistics analyses; PS: project initiator: isolation & genetic analysis of the SGD mutants, manuscript writing; SB: experimentation, experiments conceptualization, manuscript writing, project leader.

Funding

This work was funded by Université Paris Cité intramural funding. Genome sequencing was made possible by grant PSUD/SAIC N°9283-0 to P. Silar. S. Brun was supported by IdEx Université Paris Cité: ANR-18-IDEX-0001

Conflict of interest:

The authors declare that there are no conflict of interest neither commercial affiliations.

Bibliography

Asakura, M., Okuno, T., and Takano, Y. (2006). Multiple Contributions of Peroxisomal Metabolic Function to Fungal Pathogenicity in Colletotrichum lagenarium. Appl. Environ. Microbiol. *72*, 6345–6354. https://doi.org/10.1128/AEM.00988-06.

Ast, J., Stiebler, A., Freitag, J., and Bölker, M. (2013). Dual targeting of peroxisomal proteins. Frontiers in Physiology *4*. .

Baltussen, T.J.H., Zoll, J., Verweij, P.E., and Melchers, W.J.G. (2020). Molecular Mechanisms of Conidial Germination in Aspergillus spp. Microbiol. Mol. Biol. Rev. *84*. https://doi.org/10.1128/MMBR.00049-19.

Benson, D.A., Cavanaugh, M., Clark, K., Karsch-Mizrachi, I., Lipman, D.J., Ostell, J., and Sayers, E.W. (2013). GenBank. Nucleic Acids Res *41*, D36-42. https://doi.org/10.1093/nar/gks1195.

Berteaux-Lecellier, V., Picard, M., Thompson-Coffe, C., Zickler, D., Panvier-Adoutte, A., and Simonet, J.-M. (1995). A nonmammalian homolog of the PAF7 gene(Zellweger syndrome) discovered as a gene involved in caryogamy in the fungus Podospora anserina. Cell *81*, 1043–1051. https://doi.org/10.1016/S0092-8674(05)80009-1.

bioRxiv preprint doi: https://doi.org/10.1101/2022.04.08.487612; this version posted April 10, 2022. The copyright holder for this preprint (which was not certified by peer review) is the author/funder, who has granted bioRxiv a license to display the preprint in perpetuity. It is made available under aCC-BY-NC-ND 4.0 International license.

Bhambra, G.K., Wang, Z.-Y., Soanes, D.M., Wakley, G.E., and Talbot, N.J. (2006). Peroxisomal carnitine acetyl transferase is required for elaboration of penetration hyphae during plant infection by *Magnaporthe grisea*: Carnitine metabolism in *Magnaporthe*. Molecular Microbiology *61*, 46–60. https://doi.org/10.1111/j.1365-2958.2006.05209.x.

Boisnard, S., Espagne, E., Zickler, D., Bourdais, A., Riquet, A.-L., and Berteaux-Lecellier, V. (2009). Peroxisomal ABC transporters and β-oxidation during the life cycle of the filamentous fungus Podospora anserina. Fungal Genetics and Biology *46*, 55–66. https://doi.org/10.1016/j.fgb.2008.10.006.

Bonnet, C., Espagne, E., Zickler, D., Boisnard, S., Bourdais, A., and Berteaux-Lecellier, V. (2006). The peroxisomal import proteins PEX2, PEX5 and PEX7 are differently involved in Podospora anserina sexual cycle. Molecular Microbiology *62*, 157–169. https://doi.org/10.1111/j.1365-2958.2006.05353.x.

Brocard, C., and Hartig, A. (2006). Peroxisome targeting signal 1: Is it really a simple tripeptide? Biochimica et Biophysica Acta (BBA) - Molecular Cell Research *1763*, 1565–1573. https://doi.org/10.1016/j.bbamcr.2006.08.022.

Brun, S., and Silar, P. (2010). Convergent Evolution of Morphogenetic Processes in Fungi. In Evolutionary Biology – Concepts, Molecular and Morphological Evolution, P. Pontarotti, ed. (Springer Berlin Heidelberg), pp. 317–328.

Brun, S., Malagnac, F., Bidard, F., Lalucque, H., and Silar, P. (2009). Functions and regulation of the Nox family in the filamentous fungus *Podospora anserina* : a new role in cellulose degradation. Molecular Microbiology *74*, 480–496. https://doi.org/10.1111/j.1365-2958.2009.06878.x.

Cano-Dominguez, N., Alvarez-Delfin, K., Hansberg, W., and Aguirre, J. (2008). NADPH Oxidases NOX-1 and NOX-2 Require the Regulatory Subunit NOR-1 To Control Cell Differentiation and Growth in Neurospora crassa. Eukaryotic Cell *7*, 1352–1361. https://doi.org/10.1128/EC.00137-08.

Chen, X.-L., Wang, Z., and Liu, C. (2016). Roles of Peroxisomes in the Rice Blast Fungus.

Choi, Y., and Chan, A.P. (2015). PROVEAN web server: a tool to predict the functional effect of amino acid substitutions and indels. Bioinformatics *31*, 2745–2747. https://doi.org/10.1093/bioinformatics/btv195.

Choi, Y., Sims, G.E., Murphy, S., Miller, J.R., and Chan, A.P. (2012). Predicting the Functional Effect of Amino Acid Substitutions and Indels. PLOS ONE *7*, e46688. https://doi.org/10.1371/journal.pone.0046688.

Coppin, E., and Silar, P. (2007). Identification of PaPKS1, a polyketide synthase involved in melanin formation and its use as a genetic tool in Podospora anserina. Mycological Research *111*, 901–908. https://doi.org/10.1016/j.mycres.2007.05.011.

Dagdas, Y.F., Yoshino, K., Dagdas, G., Ryder, L.S., Bielska, E., Steinberg, G., and Talbot, N.J. (2012). Septin-Mediated Plant Cell Invasion by the Rice Blast Fungus, Magnaporthe oryzae. Science *336*, 1590–1595. https://doi.org/10.1126/science.1222934.

Daverdin, G., Rouxel, T., Gout, L., Aubertot, J.-N., Fudal, I., Meyer, M., Parlange, F., Carpezat, J., and Balesdent, M.-H. (2012). Genome Structure and Reproductive Behaviour Influence the Evolutionary Potential of a Fungal Phytopathogen. PLoS Pathog *8*. https://doi.org/10.1371/journal.ppat.1003020.

bioRxiv preprint doi: https://doi.org/10.1101/2022.04.08.487612; this version posted April 10, 2022. The copyright holder for this preprint (which was not certified by peer review) is the author/funder, who has granted bioRxiv a license to display the preprint in perpetuity. It is made available under aCC-BY-NC-ND 4.0 International license.

Demoor, A., Silar, P., and Brun, S. (2019). Appressorium: The Breakthrough in Dikarya. J Fungi (Basel) *5*. https://doi.org/10.3390/jof5030072.

Dirschnabel, D.E., Nowrousian, M., Cano-Dominguez, N., Aguirre, J., Teichert, I., and Kuck, U. (2014). New Insights Into the Roles of NADPH Oxidases in Sexual Development and Ascospore Germination in Sordaria macrospora. Genetics *196*, 729–744. https://doi.org/10.1534/genetics.113.159368.

Elgersma, Y., van Roermund, C.W., Wanders, R.J., and Tabak, H.F. (1995). Peroxisomal and mitochondrial carnitine acetyltransferases of Saccharomyces cerevisiae are encoded by a single gene. EMBO J *14*, 3472–3479. .

El-Khoury, R., Sellem, C.H., Coppin, E., Boivin, A., Maas, M.F.P.M., Debuchy, R., and Sainsard-Chanet, A. (2008). Gene deletion and allelic replacement in the filamentous fungus <Emphasis Type="Italic">Podospora anserina</Emphasis>. Curr Genet *53*, 249–258. https://doi.org/10.1007/s00294-008-0180-3.

Espagne, E., Lespinet, O., Malagnac, F., Da Silva, C., Jaillon, O., Porcel, B.M., Couloux, A., Aury, J.-M., Ségurens, B., Poulain, J., et al. (2008). The genome sequence of the model ascomycete fungus Podospora anserina. Genome Biology *9*, R77. .

Faure, G., and Koonin, E.V. (2015). Universal distribution of mutational effects on protein stability, uncoupling of protein robustness from sequence evolution and distinct evolutionary modes of prokaryotic and eukaryotic proteins. Phys Biol *12*, 035001. https://doi.org/10.1088/1478-3975/12/3/035001.

Fukasawa, Y., Tsuji, J., Fu, S.-C., Tomii, K., Horton, P., and Imai, K. (2015). MitoFates: improved prediction of mitochondrial targeting sequences and their cleavage sites. Mol Cell Proteomics *14*, 1113–1126. https://doi.org/10.1074/mcp.M114.043083.

Funahashi, J., Sugita, Y., Kitao, A., and Yutani, K. (2003). How can free energy component analysis explain the difference in protein stability caused by amino acid substitutions? Effect of three hydrophobic mutations at the 56th residue on the stability of human lysozyme. Protein Eng *16*, 665–671. https://doi.org/10.1093/protein/gzg083.

Gautier, V., Levert, E., Giraud, T., and Silar, P. (2021). Important role of melanin for fertility in the fungus Podospora anserina. G3 Genes|Genomes|Genetics https://doi.org/10.1093/g3journal/jkab159.

Gómez, B.L., and Nosanchuk, J.D. (2003). Melanin and fungi. Current Opinion in Infectious Diseases *16*, 91–96. .

Grigoriev, I.V., Nikitin, R., Haridas, S., Kuo, A., Ohm, R., Otillar, R., Riley, R., Salamov, A., Zhao, X., Korzeniewski, F., et al. (2014). MycoCosm portal: gearing up for 1000 fungal genomes. Nucleic Acids Research *42*, D699–D704. https://doi.org/10.1093/nar/gkt1183.

Grognet, P., Lalucque, H., Malagnac, F., and Silar, P. (2014). Genes That Bias Mendelian Segregation. PLOS Genetics *10*, e1004387. https://doi.org/10.1371/journal.pgen.1004387.

Guindon, S., and Gascuel, O. (2003). A simple, fast, and accurate algorithm to estimate large phylogenies by maximum likelihood. Syst Biol *52*, 696–704. https://doi.org/10.1080/10635150390235520.

Hoekstra, R.F. (2005). Why sex is good. Nature *434*, 571–573. https://doi.org/10.1038/434571a.

bioRxiv preprint doi: https://doi.org/10.1101/2022.04.08.487612; this version posted April 10, 2022. The copyright holder for this preprint (which was not certified by peer review) is the author/funder, who has granted bioRxiv a license to display the preprint in perpetuity. It is made available under aCC-BY-NC-ND 4.0 International license.

Hooks, K.B., Turner, J.E., Graham, I.A., Runions, J., and Hooks, M.A. (2012). GFP-tagging of Arabidopsis acyl-activating enzymes raises the issue of peroxisome-chloroplast import competition versus dual localization. J Plant Physiol *169*, 1631–1638. https://doi.org/10.1016/j.jplph.2012.05.026.

Horton, P., Park, K.-J., Obayashi, T., Fujita, N., Harada, H., Adams-Collier, C.J., and Nakai, K. (2007). WoLF PSORT: protein localization predictor. Nucleic Acids Res *35*, W585-587. https://doi.org/10.1093/nar/gkm259.

Howlett, B.J., Idnurm, A., and Pedras, M.S.C. (2001). Leptosphaeria maculans, the Causal Agent of Blackleg Disease of Brassicas. Fungal Genetics and Biology *33*, 1–14. https://doi.org/10.1006/fgbi.2001.1274.

Hynes, M.J., Murray, S.L., Andrianopoulos, A., and Davis, M.A. (2011). Role of Carnitine Acetyltransferases in Acetyl Coenzyme A Metabolism in Aspergillus nidulans. Eukaryotic Cell *10*, 547–555. https://doi.org/10.1128/EC.00295-10.

Imazaki, A., Tanaka, A., Harimoto, Y., Yamamoto, M., Akimitsu, K., Park, P., and Tsuge, T. (2010). Contribution of Peroxisomes to Secondary Metabolism and Pathogenicity in the Fungal Plant Pathogen Alternaria alternata. Eukaryotic Cell *9*, 682–694. https://doi.org/10.1128/EC.00369-09.

Katoh, K., Kuma, K., Toh, H., and Miyata, T. (2005). MAFFT version 5: improvement in accuracy of multiple sequence alignment. Nucleic Acids Res *33*, 511–518. https://doi.org/10.1093/nar/gki198.

Kawamoto, S., Ueda, M., Nozaki, C., Yamamura, M., Tanaka, A., and Fukui, S. (1978). Localization of carnitine acetyltransferase in peroxisomes and in mitochondria of n-alkane-grown candida tropicalis. FEBS Letters *96*, 37–40. https://doi.org/10.1016/0014-5793(78)81057-6.

Kretschmer, M., Wang, J., and Kronstad, J.W. (2012). Peroxisomal and Mitochondrial β-Oxidation Pathways Influence the Virulence of the Pathogenic Fungus Cryptococcus neoformans. Eukaryotic Cell *11*, 1042–1054. https://doi.org/10.1128/EC.00128-12.

Kriventseva, E.V., Kuznetsov, D., Tegenfeldt, F., Manni, M., Dias, R., Simão, F.A., and Zdobnov, E.M. (2019). OrthoDB v10: sampling the diversity of animal, plant, fungal, protist, bacterial and viral genomes for evolutionary and functional annotations of orthologs. Nucleic Acids Res *47*, D807–D811. https://doi.org/10.1093/nar/gky1053.

Lalucque, H., Malagnac, F., Brun, S., Kicka, S., and Silar, P. (2012). A Non-Mendelian MAPK-Generated Hereditary Unit Controlled by a Second MAPK Pathway in Podospora anserina. Genetics *191*, 419–433. https://doi.org/10.1534/genetics.112.139469.

Lambou, K., Malagnac, F., Barbisan, C., Tharreau, D., Lebrun, M.-H., and Silar, P. (2008). The Crucial Role of the Pls1 Tetraspanin during Ascospore Germination in Podospora anserina Provides an Example of the Convergent Evolution of Morphogenetic Processes in Fungal Plant Pathogens and Saprobes. Eukaryotic Cell *7*, 1809–1818. https://doi.org/10.1128/EC.00149-08.

Langfelder, K., Streibel, M., Jahn, B., Haase, G., and Brakhage, A.A. (2003). Biosynthesis of fungal melanins and their importance for human pathogenic fungi. Fungal Genetics and Biology *38*, 143–158. https://doi.org/10.1016/S1087-1845(02)00526-1.

Lecellier, G., and Silar, P. (1994). Rapid methods for nucleic acids extraction from Petri dish-grown mycelia. Curr Genet *25*, 122–123. https://doi.org/10.1007/BF00309536.

bioRxiv preprint doi: https://doi.org/10.1101/2022.04.08.487612; this version posted April 10, 2022. The copyright holder for this preprint (which was not certified by peer review) is the author/funder, who has granted bioRxiv a license to display the preprint in perpetuity. It is made available under aCC-BY-NC-ND 4.0 International license.

Letunic, I., and Bork, P. (2007). Interactive Tree Of Life (iTOL): an online tool for phylogenetic tree display and annotation. Bioinformatics *23*, 127–128. https://doi.org/10.1093/bioinformatics/btl529.

Li, D., Bobrowicz, P., Wilkinson, H.H., and Ebbole, D.J. (2005). A Mitogen-Activated Protein Kinase Pathway Essential for Mating and Contributing to Vegetative Growth in Neurospora crassa. Genetics *170*, 1091–1104. https://doi.org/10.1534/genetics.104.036772.

Liberti, D., Rollins, J.A., and Dobinson, K.F. (2013). Peroxysomal Carnitine Acetyl Transferase Influences Host Colonization Capacity in Sclerotinia sclerotiorum. MPMI *26*, 768–780. https://doi.org/10.1094/MPMI-03-13-0075-R.

Malagnac, F., Lalucque, H., Lepère, G., and Silar, P. (2004). Two NADPH oxidase isoforms are required for sexual reproduction and ascospore germination in the filamentous fungus Podospora anserina. Fungal Genetics and Biology *41*, 982–997. https://doi.org/10.1016/j.fgb.2004.07.008.

Malagnac, F., Bidard, F., Lalucque, H., Brun, S., Lambou, K., Lebrun, M.-H., and Silar, P. (2008). Convergent evolution of morphogenetic processes in fungi. Communicative & Integrative Biology *1*, 180–181. https://doi.org/10.4161/cib.1.2.7198.

Marchler-Bauer, A., and Bryant, S.H. (2004). CD-Search: protein domain annotations on the fly. Nucleic Acids Res *32*, W327–W331. https://doi.org/10.1093/nar/gkh454.

Masterson, C., and Wood, C. (2000). Pea chloroplast carnitine acetyltransferase. Proceedings of the Royal Society of London. Series B: Biological Sciences *267*, 1–6. https://doi.org/10.1098/rspb.2000.0958.

Nolting, N., and Pöggeler, S. (2006). A STE12 homologue of the homothallic ascomycete Sordaria macrospora interacts with the MADS box protein MCM1 and is required for ascosporogenesis. Molecular Microbiology *62*, 853–868. https://doi.org/10.1111/j.1365-2958.2006.05415.x.

Osherov, N., and May, G.S. (2001). The molecular mechanisms of conidial germination. FEMS Microbiol Lett *199*, 153–160. https://doi.org/10.1111/j.1574-6968.2001.tb10667.x.

Pandey, A., Roca, M.G., Read, N.D., and Glass, N.L. (2004). Role of a Mitogen-Activated Protein Kinase Pathway during Conidial Germination and Hyphal Fusion in Neurospora crassa. Eukaryotic Cell *3*, 348–358. https://doi.org/10.1128/EC.3.2.348-358.2004.

Peraza Reyes, L., and Berteaux-Lecellier, V. (2013). Peroxisomes and sexual development in fungi. Frontiers in Physiology *4*. .

Peraza-Reyes, L., Zickler, D., and Berteaux-Lecellier, V. (2008). The Peroxisome RING-Finger Complex is Required for Meiocyte Formation in the Fungus Podospora anserina. Traffic *9*, 1998–2009. https://doi.org/10.1111/j.1600-0854.2008.00812.x.

Peraza-Reyes, L., Arnaise, S., Zickler, D., Coppin, E., Debuchy, R., and Berteaux-Lecellier, V. (2011). The importomer peroxins are differentially required for peroxisome assembly and meiotic development in Podospora anserina: insights into a new peroxisome import pathway. Molecular Microbiology *82*, 365–377. https://doi.org/10.1111/j.1365-2958.2011.07816.x.

Quan, L., Lv, Q., and Zhang, Y. (2016). STRUM: structure-based prediction of protein stability changes upon single-point mutation. Bioinformatics *32*, 2936–2946. https://doi.org/10.1093/bioinformatics/btw361.

bioRxiv preprint doi: https://doi.org/10.1101/2022.04.08.487612; this version posted April 10, 2022. The copyright holder for this preprint (which was not certified by peer review) is the author/funder, who has granted bioRxiv a license to display the preprint in perpetuity. It is made available under aCC-BY-NC-ND 4.0 International license.

Quevillon, E., Silventoinen, V., Pillai, S., Harte, N., Mulder, N., Apweiler, R., and Lopez, R. (2005). InterProScan: protein domains identifier. Nucleic Acids Res *33*, W116-120. https://doi.org/10.1093/nar/gki442.

Ramos-Pamplona, M., and Naqvi, N.I. (2006). Host invasion during rice-blast disease requires carnitine-dependent transport of peroxisomal acetyl-CoA: Carnitine metabolism and rice-blast. Molecular Microbiology *61*, 61–75. https://doi.org/10.1111/j.1365-2958.2006.05194.x.

Rizet, G. (1952). Les phénomènes de barrage chez Podospora anserina. I. Analyse génétique des barrages entre souches S et s. Revue de Cytologie et de Biologie Végétale *13*, 51–92. .

Rizet, G., and Engelmann, C. (1949). Contribution à l'étude génétique d'un Ascomycète tétrasporé: Podospora anserina. Revue de Cytologie et de Biologie Végétale *11*, 201–304. .

van Roermund, C.W.T., Hettema, E.H., van den Berg, M., Tabak, H.F., and Wanders, R.J.A. (1999). Molecular characterization of carnitine-dependent transport of acetyl-CoA from peroxisomes to mitochondria in Saccharomyces cerevisiae and identification of a plasma membrane carnitine transporter, Agp2p. The EMBO Journal *18*, 5843–5852. https://doi.org/10.1093/emboj/18.21.5843.

Roy, A., Kucukural, A., and Zhang, Y. (2010). I-TASSER: a unified platform for automated protein structure and function prediction. Nat Protoc *5*, 725–738. https://doi.org/10.1038/nprot.2010.5.

Ruprich-Robert, G., Berteaux-Lecellier, V., Zickler, D., Panvier-Adoutte, A., and Picard, M. (2002). Identification of Six Loci in Which Mutations Partially Restore Peroxisome Biogenesis and/or Alleviate the Metabolic Defect of pex2 Mutants in Podospora. Genetics *161*, 1089–1099. .

Ryder, L.S., Dagdas, Y.F., Mentlak, T.A., Kershaw, M.J., Thornton, C.R., Schuster, M., Chen, J., Wang, Z., and Talbot, N.J. (2013). NADPH oxidases regulate septin-mediated cytoskeletal remodeling during plant infection by the rice blast fungus. Proceedings of the National Academy of Sciences *110*, 3179–3184. https://doi.org/10.1073/pnas.1217470110.

Ryder, L.S., Dagdas, Y.F., Kershaw, M.J., Venkataraman, C., Madzvamuse, A., Yan, X., Cruz-Mireles, N., Soanes, D.M., Oses-Ruiz, M., Styles, V., et al. (2019). A sensor kinase controls turgor-driven plant infection by the rice blast fungus. Nature *574*, 423–427. https://doi.org/10.1038/s41586-019-1637-x.

Seccombe, D.W., and Hahn, P. (1980). Carnitine Acetyltransferase in Developing Mammals. NEO *38*, 90–95. https://doi.org/10.1159/000241347.

Sellem, C.H., Marsy, S., Boivin, A., Lemaire, C., and Sainsard-Chanet, A. (2007). A mutation in the gene encoding cytochrome c1 leads to a decreased ROS content and to a long-lived phenotype in the filamentous fungus Podospora anserina. Fungal Genetics and Biology *44*, 648–658. https://doi.org/10.1016/j.fgb.2006.09.005.

Sigrist, C.J.A., Cerutti, L., de Castro, E., Langendijk-Genevaux, P.S., Bulliard, V., Bairoch, A., and Hulo, N. (2010). PROSITE, a protein domain database for functional characterization and annotation. Nucleic Acids Res *38*, D161–D166. https://doi.org/10.1093/nar/gkp885.

Silar, P. (1995). Two new easy to use vectors for transformations. Fungal Genetics Reports *42*, 73. https://doi.org/10.4148/1941-4765.1353.

Silar, P. (2013). Podospora anserina: From Laboratory to Biotechnology. In Genomics of Soil- and Plant-Associated Fungi, B.A. Horwitz, P.K. Mukherjee, M. Mukherjee, and C.P. Kubicek, eds. (Berlin, Heidelberg: Springer Berlin Heidelberg), pp. 283–309.

bioRxiv preprint doi: https://doi.org/10.1101/2022.04.08.487612; this version posted April 10, 2022. The copyright holder for this preprint (which was not certified by peer review) is the author/funder, who has granted bioRxiv a license to display the preprint in perpetuity. It is made available under aCC-BY-NC-ND 4.0 International license.

Silar, P. (2020). Podospora anserina.

Son, H., Min, K., Lee, J., Choi, G.J., Kim, J.-C., and Lee, Y.-W. (2012). Mitochondrial Carnitine-Dependent Acetyl Coenzyme A Transport Is Required for Normal Sexual and Asexual Development of the Ascomycete Gibberella zeae. Eukaryotic Cell *11*, 1143–1153. https://doi.org/10.1128/EC.00104-12.

Strijbis, K., and Distel, B. (2010). Intracellular Acetyl Unit Transport in Fungal Carbon Metabolism. Eukaryotic Cell *9*, 1809–1815. https://doi.org/10.1128/EC.00172-10.

Strijbis, K., Vaz, F.M., and Distel, B. (2010). Enzymology of the carnitine biosynthesis pathway. IUBMB Life *62*, 357–362. https://doi.org/10.1002/iub.323.

Sweigard, J.A., Carroll, A.M., Farrall, L., Chumley, F.G., and Valent, B. (1998). Magnaporthe grisea Pathogenicity Genes Obtained Through Insertional Mutagenesis. MPMI *11*, 404–412. https://doi.org/10.1094/MPMI.1998.11.5.404.

Swiegers, J.H., Dippenaar, N., Pretorius, I.S., and Bauer, F.F. (2001). Carnitine-dependent metabolic activities in Saccharomyces cerevisiae: three carnitine acetyltransferases are essential in a carnitine-dependent strain. Yeast *18*, 585–595. https://doi.org/10.1002/yea.712.

Trapero-Casas, A., and Kaiser, W.J. (2007). Differences Between Ascospores and Conidia of Didymella rabiei in Spore Germination and Infection of Chickpea. Phytopathology® *97*, 1600–1607. https://doi.org/10.1094/PHYTO-97-12-1600.

Wang, Z.-Y., Soanes, D.M., Kershaw, M.J., and Talbot, N.J. (2007). Functional Analysis of Lipid Metabolism in Magnaporthe grisea Reveals a Requirement for Peroxisomal Fatty Acid β-Oxidation During Appressorium-Mediated Plant Infection. MPMI *20*, 475–491. https://doi.org/10.1094/MPMI-20-5-0475.

Waterhouse, A., Bertoni, M., Bienert, S., Studer, G., Tauriello, G., Gumienny, R., Heer, F.T., de Beer, T.A.P., Rempfer, C., Bordoli, L., et al. (2018). SWISS-MODEL: homology modelling of protein structures and complexes. Nucleic Acids Res *46*, W296–W303. https://doi.org/10.1093/nar/gky427.

Waterhouse, A.M., Procter, J.B., Martin, D.M.A., Clamp, M., and Barton, G.J. (2009). Jalview Version 2--a multiple sequence alignment editor and analysis workbench. Bioinformatics *25*, 1189–1191. https://doi.org/10.1093/bioinformatics/btp033.

Widmann, C., Gibson, S., Jarpe, M.B., and Johnson, G.L. (1999). Mitogen-Activated Protein Kinase: Conservation of a Three-Kinase Module From Yeast to Human. Physiological Reviews *79*, 143–180. .

Xu, J.-R., Staiger, C.J., and Hamer, J.E. (1998). Inactivation of the mitogen-activated protein kinase Mps1 from the rice blast fungus prevents penetration of host cells but allows activation of plant defense responses. PNAS *95*, 12713–12718. https://doi.org/10.1073/pnas.95.21.12713.

Zhou, H., and Lorenz, M.C. (2008). Carnitine acetyltransferases are required for growth on non-fermentable carbon sources but not for pathogenesis in Candida albicans. Microbiology (Reading, Engl.) *154*, 500–509. https://doi.org/10.1099/mic.0.2007/014555-0.

bioRxiv preprint doi: https://doi.org/10.1101/2022.04.08.487612; this version posted April 10, 2022. The copyright holder for this preprint (which was not certified by peer review) is the author/funder, who has granted bioRxiv a license to display the preprint in perpetuity. It is made available under aCC-BY-NC-ND 4.0 International license.

STRAIN	GENOTYPE	MARKER	REFERENCE
Wild-Type	*big "S"*	none	(Rizet and Engelmann, 1949)
Δmus51	*Δmus51::phleoR*	phleoR	
Δmus51	*Δmus51::genR*	genR	
Δmus52	*Δmus52::genR*	genR	
PaMKK2^{c}	*PaMKK2^{c}::phleoR*	phleoR	(Lalucque et al., 2012)
PaMpk2	*PaMpk2::hygR*	hygR	(Lalucque et al., 2012)
PaNox2	*PaNox2::phleoR*	phleoR	(Malagnac et al., 2004)
PaPls1	*PaPls1::hygR*	hygR	(Lambou et al., 2008)
PaPks1^{193}	*PaPks1^{193}*	none	(Coppin and Silar, 2007)
PaPks1^{136}	*PaPks1^{136}*	none	(Coppin and Silar, 2007)
mito-GFP	*mito-GFP-hygR*	hygR	(Sellem et al., 2007)
GFP-SKL	*GFP-SKL-phleoR*	phleoR	(Ruprich-Robert et al., 2002)
ΔPex5	*ΔPex5::hygR*	hygR	(Bonnet et al., 2006)
ΔPex7	*ΔPex7::phleoR*	phleoR	(Bonnet et al., 2006)
ΔPex13	*ΔPex13::hygR*	hygR	(Peraza-Reyes et al., 2011)
GUN1^{SG}	*GUN1^{I441N}*	none	This study
GUN1^{SG} pGUN1	*GUN1^{SG} pBC-GUN1-genR*	genR	
ΔGUN1	*ΔPa_6_1340::hygR*	hygR	
ΔGUN1 pGUN1	*ΔPa_6_1340::hygR pBC-GUN1-genR*	hygR, phleoR	
ΔGUP1	*ΔPa_3_7660::phleoR*	phleoR	
ΔGUP1 pGUP1	*ΔPa_3_7660::phleoR pBC-GUP1-nouR*	phleoR, nouR	
ΔGUN1 ΔGUP1	*ΔPa_6_1340::hygR ΔPa_3_7660::phleoR*	hygR, phleoR	
ΔGUN1 ΔGUP1 pGUN1	*ΔPa_6_1340::hygR ΔPa_3_7660::phleoR pBC-GUN1-genR*	hygR, phleoR, genR	
GUN1-mCherry	*GUN1::mCherry-hygR*	hygR	
GUN1-mCherry GFP-SKL	*GUN1::mCherry-hygR GFP-SKL-phleoR*	hygR, phleoR	
GUN1-mCherry mito-GFP	*GUN1::mCherry-hygR mito-GFP-hygR*	hygR	
GUN1-mCherry-AKI	*GUN1::mCherry-AKI-nouR*	nouR	
GUN1-mCherry-AKI GFP-SKL	*GUN1::mCherry-AKI-nouR GFP-SKL-phleoR*	phleoR, nouR	
GUN1-mCherry-AKI mito-GFP	*GUN1::mCherry-AKI-nouR mito-GFP-hygR*	hygR, nouR	
GUN1^{SG}-mCherry	*GUN1^{SG}::mCherry-hygR*	hygR	
GUN1^{SG}-mCherry GFP-SKL	*GUN1^{SG}::mCherry-hygR GFP-SKL-phleoR*	hygR, phleoR	
GUN1^{SG}-mCherry mito-GFP	*GUN1^{SG}::mCherry-hygR mito-GFP-hygR*	hygR	
GUN1^{SG}-mCherry-AKI	*GUN1^{SG}::mCherry-AKI-nourR*	nouR	
GUN1^{SG}-mCherry-AKI GFP-SKL	*GUN1^{SG}::mCherry-AKI-nouR GFP-SKL-phleoR*	phleoR, nouR	
GUN1^{SG}-mCherry-AKI mito-GFP	*GUN1^{SG}::mCherry-AKI-nouR mito-GFP-hygR*	hygR, nouR	
PaPks1^{136} GUN1-mCherry mito-GFP	*PaPks1^{136} GUN1::mCherry-hygR mito-GFP-hygR*	hygR	
PaPks1^{136} GUN1-mCherry-AKI GFP-SKL	*PaPks1^{136} GUN1::mCherry-AKI-nouR GFP-SKL-phleoR*	phleoR, nouR	
PaPks1^{136} GUN1-mCherry-AKI mito-GFP	*PaPks1^{136} GUN1::mCherry-AKI-nouR mito-GFP::hygR*	hygR, nouR	
PaPks1^{136} GUN1-mCherry GFP-SKL	*PaPks1^{136} GUN1::mCherry-hygR GFP-SKL-phleoR*	hygR, phleoR	
PaPks1^{136} GUN1^{SG}-mCherry GFP-SKL	*PaPks1^{136} GUN1^{SG}::mCherry-hygR GFP-SKL-phleoR*	hygR, phleoR	
PaPks1^{136} GUN1^{SG}-mCherry mito-GFP	*PaPks1^{136} GUN1^{SG}::mCherry-hygR mito-GFP-hygR*	hygR	
PaPks1^{136} GUN1^{SG}-mCherry-AKI GFP-SKL	*PaPks1^{136} GUN1^{SG}::mCherry-AKI-nouR GFP-SKL-phleoR*	phleoR, nouR	
PaPks1^{136} GUN1^{SG}-mCherry-AKI mito-GFP	*PaPks1^{136} GUN1^{SG}::mCherry-AKI-nouR mito-GFP-hygR*	hygR, nouR	
GUN1^{SG} ΔPex7	*GUN1^{SG} ΔPex7::phleoR*	phleoR	
PaMkk2^{c} ΔGUN1	*PaMkk2^{c}-phleoR ΔPa_6_1340::hygR*	hygR phleoR	

Table 1: Strains list

bioRxiv preprint doi: https://doi.org/10.1101/2022.04.08.487612; this version posted April 10, 2022. The copyright holder for this preprint (which was not certified by peer review) is the author/funder, who has granted bioRxiv a license to display the preprint in perpetuity. It is made available under aCC-BY-NC-ND 4.0 International license.

Strains	**day**
WT	2
GUN1^{SG}	3
ΔGUN1	4
ΔGUP1	2
ΔGUN1ΔGUP1	4

Table 2: Cellophane penetration assay. The listed strains were cultured for 5 days on M2 medium topped with a cellophane layer at 27 °C. After 2-, 3-, 4- and 5-days of culture, the cellophane layer was removed to check fungal growth in the medium underneath. The day the cellophane was breached is indicated. 3 replicates were made for each day of culture. This experiment was repeated twice.

M2			**G+YE**		
[genR]	[genS]	Total	[genR]	[genS]	Total:
Ø	11	42	18	13	42

Table 3 : *GUN1^{SG}* X *GUN1^{SG} pGUN1* (*pBC-GUN1-genR*). 42 homokaryotic ascospores were sown on both M2 and G+YE media. The numbers correspond to the amount of germinated spores.

GUN1^{SG} X ΔPaPls1::hygR			***GUN1^{SG} X ΔPaNox2::phleoR***			***GUN1^{SG} X ΔPaMpk2::hygR***		
[hygR]	[hygS]	Total:	[phleoR]	[phleoS]	Total:	[hygR]	[hygS]	Total:
Ø	20	48	Ø	13	48	Ø	26	48

Table 4: Results of the crosses between *GUN1^{SG}* and *ΔPaPls1, ΔPaNox2, ΔPaMpk2*. 48 homokaryotic ascospores were sown on G+YE medium for each cross. The numbers correspond to the amount of germinated spores.

bioRxiv preprint doi: https://doi.org/10.1101/2022.04.08.487612; this version posted April 10, 2022. The copyright holder for this preprint (which was not certified by peer review) is the author/funder, who has granted bioRxiv a license to display the preprint in perpetuity. It is made available under aCC-BY-NC-ND 4.0 International license.

[hygR, phleoS] *ΔGUN1*	[hygR, phleoR] *ΔGUN1 PaMKK2^{C}*	[hygS, phleoR] *GUN1 PaMKK2^{C}*	[hygS, phleoS] *GUN1*	Total:
0	26	14	0	40

Table 5: *PaMKK2^{C}::phleoR* X *ΔGUN1::hygR*. 40 homokaryotic ascospores were sown on M2 medium and genotyped.

ΔPex7 GUN1^{SG} [hygS, phleoR]	*GUN1^{SG}* [hygS, phleoS]	*+* [hygS, phleoS]	*ΔPex5 GUN1^{SG}* [hygR, phleoS]	*ΔPex5* [hygR, phleoS]	*ΔPex5 ΔPex7* [hygR, phleoR]	*ΔPex7* [hygS, phleoR]	*ΔPex5 ΔPex7 GUN1^{SG}* [hygR, phleoR]	Total
15*	7*	4	0	0	0	0	0	75

Table 6: *ΔPex5 ΔPex7* (*ΔPex5::hygR ΔPex7::phleoR*) *X GUN1^{SG}*. 75 homokaryotic ascospores were sown on G+YE medium. *, ascospores of this genotype show spontaneous germination on standard M2 medium.

GUN1^{SG} [HygS]	*+* [hygS]	*ΔPex13* [hygR]	*ΔPex13 GUN1^{SG}* [hygR]	Total
14*	5	0	0	64

Table 7: *ΔPex13 (ΔPex13::hygR) X GUN1^{SG}*. 64 homokaryotic ascospores were sown on G+YE medium. *, ascospores of this genotype show spontaneous germination on standard M2 medium.

bioRxiv preprint doi: https://doi.org/10.1101/2022.04.08.487612; this version posted April 10, 2022. The copyright holder for this preprint (which was not certified by peer review) is the author/funder, who has granted bioRxiv a license to display the preprint in perpetuity. It is made available under aCC-BY-NC-ND 4.0 International license.

PRIMER	SEQUENCE
pBC-For	5’-CGCGCGTAATACGACTCA-3’
pBC-Rev	5’-CGCGCAATTAACCCTCAC-3’
Fluo-MCS_For	5’-GGTTCCTGGCCTTTTGCT-3’
Fluo-MCS_Rev	5’-TCCTCGCCCTTGCTCAC-3’
1340_1	5'- CAAGAGGTGCGATTGGAGGAGGAGAGGG-3'
1340_2	5’-CTATTTAACGACCCTGCCCTGAACCGCCCAACTTCTCCTAGGCAAGTGGAGC-3’
1340_3	5’-CTTACCGCTGTTGAGATCCAGTTCGATGGCTCACGGTTGAGGGATCTAACGGGGGG-3’
1340_4	5'-GGGGGTAGGAAGAGAGGAGAGAAGTGGAG -3'
1340_MkF	5’-GCTCCACTTGCCTAGGAGAAGTTGGGCGGTTCAGGGCAGGGTCGTTAAATAG-3’
1340_MkR	5’-CCGTTAGATCCCTCAACCGTGAGCCATCGAACTGGATCTCAACAGCGGTAAG-3’
7660_F1	5’-GGCTGCCAATTGGTGGGGATCTAAACGTCA-3’
7660_R2	5’-CTATTTAACGACCCTGTGAACCGTTCTTGTCAGCTGGGGTGATCTGGATTCAA-3’
7660_F3	5’-CTTACCGCTGTTGAGATCATGGCTTGGCTATTGTGATGGGAGGGGGGGAGG-3’
7660_R4	5’-TATTTCTCAGGAAAGGTGGGGAGGCGGCCA-3’
7660_MkF	5’-TTGAATCCAGATCCAGCTGACAAGAACGGTTCAGGGCAGGGTCGTTAAATAG-3’
7660_MkR	5’-CCTCCCCCTCCCATCACAGCCAAGCCATCGAACTGGATCTCAACAGCGGTAAG-3’
Vérif 5'_1340	5’-GTCTGTCCGTTGCCTCCTTA-3’
Vérif 3'_1340	5’-TCCACCTTTTGCAGCCCCC-3’
Vérif 5'_7660	5’-CGTCTTCGTTTTGGTCTTTGTC-3’
Vérif 3'_7660	5’-ATGGGATTGGTGGTGGTTTG-3’
1340GFP_F2	5’-CTCGAGTACGTGCAGATGATCATCCAGCT-3’
1340GFP_R1	5’-GGGCCCCGATCTTGGCCTTGGGCGCCTCAA-3’
mCH_AKIR1	5'- TTAGATCTTGGCCTTGTACAGCTCGTCCATGCCGCCGG-3'
Valid_Mk_5’	5'- TGAGAAGCACACGGTCAC -3'
Valid_Mk_3’	5'- TCGGGGCGAAAACTCTC -3'
1340F3	5'- GCGTGGACAGGCATTTGT -3'
1340R2	5'-ACGCCGGATCCTGATACA-3'
7660_R5	5'-TGGATTAGAACACCTGGTGGAGGAATCGC-3'

Table S2: primers list

bioRxiv preprint doi: https://doi.org/10.1101/2022.04.08.487612; this version posted April 10, 2022. The copyright holder for this preprint (which was not certified by peer review) is the author/funder, who has granted bioRxiv a license to display the preprint in perpetuity. It is made available under aCC-BY-NC-ND 4.0 International license.

Strain	dextrin	acetate	Tween 40	oleic acid
GUN1-mCherry	+	+	+	-
GUN1^{SG}-mCherry	+	+	+	-
GUN1-mCherry-AKI	+	+	+	+
GUN1^{SG}-mCherry-AKI	+	+	+	+

Table S3: Growth of mCherry and mCherry-AKI tagged strains on different carbon sources. All the media have the same composition, except for the carbon source. The Tween 40 control medium and the oleic acid medium contain 0,5% Tween 40. +, wild-type growth; -, altered growth

bioRxiv preprint doi: https://doi.org/10.1101/2022.04.08.487612; this version posted April 10, 2022. The copyright holder for this preprint (which was not certified by peer review) is the author/funder, who has granted bioRxiv a license to display the preprint in perpetuity. It is made available under aCC-BY-NC-ND 4.0 International license.

Figures caption

Figure 1: Heterokaryotic ascospores morphology & germination. A) Ascospore morphology. (*WT*) *GUN1/GUN1*, *GUN1^{SG}/GUN1^{SG}* and , *ΔGUN1/ΔGUN1 pGUN1/pGUN1* ascospores are fully melanized compared to *ΔGUN1/ΔGUN1* ascospores which are partially demelanized: Last row shows FDS ascus composed of 2 [WT] *GUN1/GUN1* and two [*ΔGUN1*] *ΔGUN1/ΔGUN1* ascospores. Scale bar 30 µm. **B) Ascospore germination.** (*WT*) *GUN1/GUN1* ascospores require G+YE medium to germinate while *GUN1^{SG}/GUN1^{SG}* and *PaPks1^{193}/PaPks1^{193}* ascospores germinate in M2 medium. Germination occurs through the germination pore located at the tip of the ascospore. 3rd row, the melanized ascorpore is of the *PaPks1/PaPks1 genotype and the non-melanized ascospore is of the PaPks1^{193}/PaPks1^{193}* genotype. Scale bar 10µm.

Figure 2: Growth on different carbon sources. Pictures were taken after 4 days of culture. All the media have same composition except for the carbon source. The Tween 40 control medium and the oleic acid medium contain 0,5% Tween 40. Scale bar 1 cm.

Figure 3: GUN1 & GUN1^{SG} protein structure. A, Schematic representation of GUN1, GUN1-mCherry and GUN1-mCherry-AKI. MTS, Mitochondrial Targeting Signal. AKI is GUN1 PTS1-Peroxisome Targeting Sequence. The I441N mutation present in GUN1^{SG} is indicated. B, GUN1 amino acid sequence. The MTS is highlighted in blue, the histidine of the catalytic site in green, the I441 in magenta and the AKI PTS1 in yellow. C, 3D structure of murine CAT (left) and 3D modelisation of GUN1 using I-TASSER modelling tool (right). The I441 is indicated by an arrow.

Figure 4: relative Carnitine-acetyltransferase (CAT) enzymatic activity in mycelial extracts. CAT activity was assayed through the spectrophotometric measure of CoA-SH produced per minute per milligram of protein in cell extracts in presence of carnitine. Activities are reported as the activity ratio of the wild-type (*WT*) *S* strain. The CAT activity means and standard deviations have been calculated on 4 to 7 biological replicates (N is indicated for each genotype). Exact Two-Sample Fisher-Pitman Permutation Test has been realized to compare CAT activities. (*) CAT activities significantly different from the *WT* (P<0,05); (**) CAT activities in complemented strains significantly different from the activity in the respective mutant strains (P<0,05).

Figure 5: Spinning disk imaging of GUN1 and GUN^{SG} subcellular localization in mycelium. GUN1 and GUN1^{SG} have been tagged with the mCherry or the mCherry-AKI (bearing GUN1 PTS1 AKI triad) fused in C-terminus. A) Every strain analyzed carry the GFP-SKL marker tagging the peroxisomes. B) Every strain carry the mito-GFP reporter tagging mitochondria. Scale bar 5 µm.

Figure 6: Spinning disc imaging of GUN1-mCherry-AKI and GUN1^{SG}-mCherry-AKI in ascospores. All the ascospores imaged carry the *PaPks1^{136}* mutation partially impairing ascospore melanisation and making ascospores transparent for fluorescence imaging. A) Every strain carry the GFP-SKL reporter tagging peroxisomes. B) Every strain carry the mito-GFP reporter tagging mitochondria. M2 liquid medium: no induction of ascospore germination. G liquid medium: ascospore germination induction. Scale bar 5 µm

bioRxiv preprint doi: https://doi.org/10.1101/2022.04.08.487612; this version posted April 10, 2022. The copyright holder for this preprint (which was not certified by peer review) is the author/funder, who has granted bioRxiv a license to display the preprint in perpetuity. It is made available under aCC-BY-NC-ND 4.0 International license.

Figure 7. Western blot analysis of PaMpk2 phosphorylation in ascospores. Proteins were extracted from genetically homogenous ascospores. Anti-p44 and anti-phospho-p44 antibodies recognizing both PaMpk1, PaMpk2 and p-PaMpk1 and p-PaMpk2 respectively were used. For ascospore germination (*WT* ind.) induction, ascospores where placed on G+YE medium for 2h before protein extraction (see Mat. & Met.). *PaMKK2*^{c} constitutive mutation induces PaMpk2 phosphorylation and spontaneous ascospore germination.

Figure 8. Regulation of ascospore germination. Breaking of dormancy is initiated by germination triggers: ammonium acetate and bactopeptone *in vitro*. The activities of the PTS1-type and PTS-2 type importomer components Pex5, Pex7 and Pex13 are required for germination. We speculate that GUN1-driven acetyl-CoA shuttling to mitochondria activates the Mpk2/Fus3 MAPK pathway which in turn activates the NADPH oxidase complex Nox2-Pls1-NoxR. Whether activation of the Nox2 complex sets up a septin ring and actin cytoskeleton rearrangement at the germination pore in a similar manner as in *M. oryzae* appressorium remains to be addressed.

bioRxiv preprint doi: https://doi.org/10.1101/2022.04.08.487612; this version posted April 10, 2022. The copyright holder for this preprint (which was not certified by peer review) is the author/funder, who has granted bioRxiv a license to display the preprint in perpetuity. It is made available under aCC-BY-NC-ND 4.0 International license.

Fig. 1: Heterokaryotic ascospores morphology & germination

A

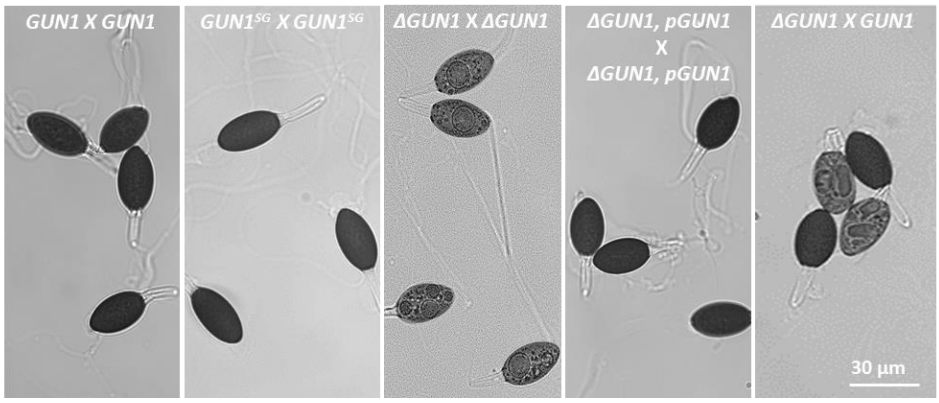

B

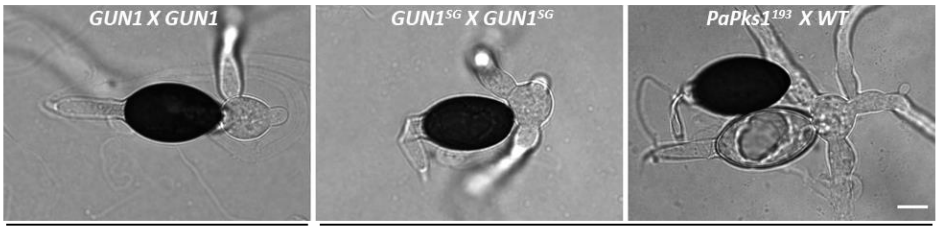

bioRxiv preprint doi: https://doi.org/10.1101/2022.04.08.487612; this version posted April 10, 2022. The copyright holder for this preprint (which was not certified by peer review) is the author/funder, who has granted bioRxiv a license to display the preprint in perpetuity. It is made available under aCC-BY-NC-ND 4.0 International license.

Fig. 2: Growth on different carbon sources

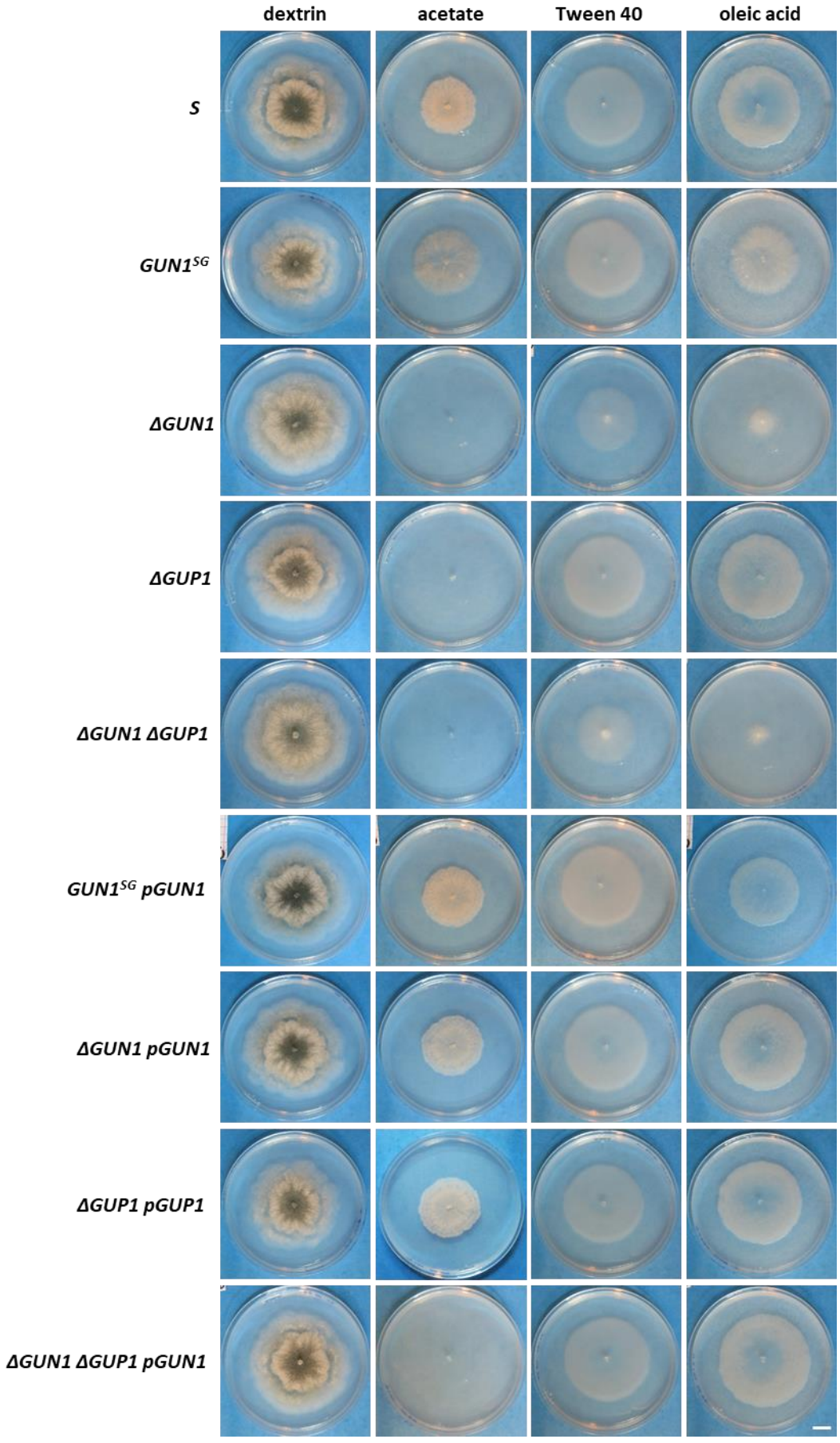

bioRxiv preprint doi: https://doi.org/10.1101/2022.04.08.487612; this version posted April 10, 2022. The copyright holder for this preprint (which was not certified by peer review) is the author/funder, who has granted bioRxiv a license to display the preprint in perpetuity. It is made available under aCC-BY-NC-ND 4.0 International license.

Fig. 3: GUN1 & GUN1^{SG} protein structures

A

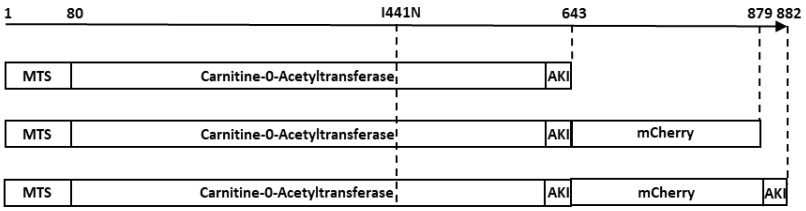

B

MFAAIARTARTEARSPALRNIIPKQTQTPLRLATMASRRNNSSLPAGYVEDKSKGPMLRFQDSLPKLPVPTLEETAARYLKS
LKPLLSPAELEKSTKAVQEFIAPNGPGRKLQEKLLARREDPKHKNWIYEWWNDAAYLSYRDPVVPYVSYFYSHRDDKRRRD
PAKRAAAITTAALEFKKQVDTGTLEPEYMKKLPICMDSYKWMFNCSRVAAKPADYPVKFDPAQNKHILVIRKNQFFKVAH
EVNGQQLNTSELEQAFRRVYELAGQRVPAVGALTSENRDVWTDARAKLLSADPKNAQSLEAIESASFVVCLDDAAPVTLE
ERAHAYWHGDGQNRWYDKPLQFIVNDNGTSGFMGEHSMMDGTPTHRLNDFVNDVIFNNKLDFADPTVRSNLPEPQV
VKFVVNKEVQSEIDRAITDFNNVIGQHQLAVQAYQGYGKGLIKKFKCSPDAYVQMIIQLAYFKMYGKNRPTYESAATRRFQ
QGRTETCRTVSEESANWCKSMADPAIPDSEKVTLFRKAIDGHLEYISAASDGKGVDRHLFGLKRLLGKGEEVPALYQDPAY
GYSSSWYLSTSQLSSEFFNGYGWSQVIDEGFGIAYMINENSLNFNIVSKGLGSEKMSYYLSEAAGEMRDLLIPTLEAPKAKI

C

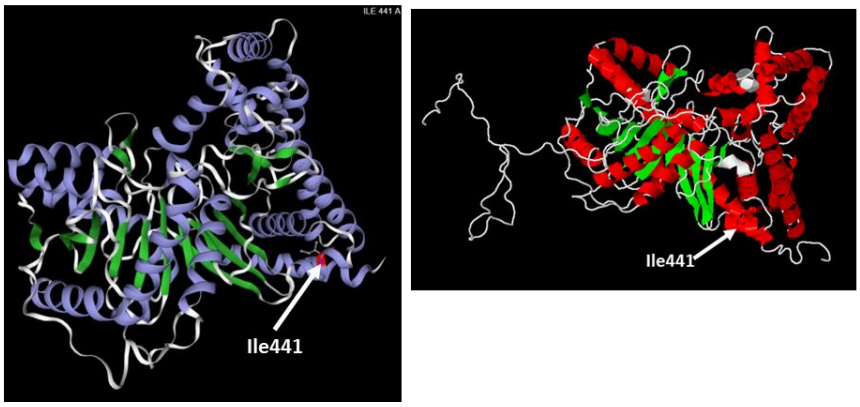

Fig. 4: relative Carnitine-acetyltransferase (CAT) enzymatic activity in mycelial extracts

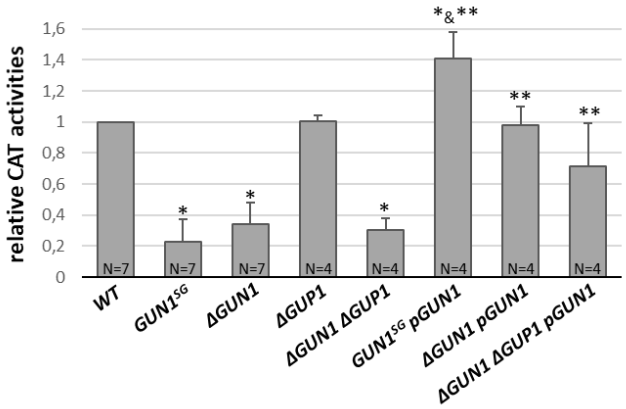

bioRxiv preprint doi: https://doi.org/10.1101/2022.04.08.487612; this version posted April 10, 2022. The copyright holder for this preprint (which was not certified by peer review) is the author/funder, who has granted bioRxiv a license to display the preprint in perpetuity. It is made available under aCC-BY-NC-ND 4.0 International license.

Fig. 5: Spinning disk imaging of GUN1 and GUN^{SG} subcellular localization in mycelium

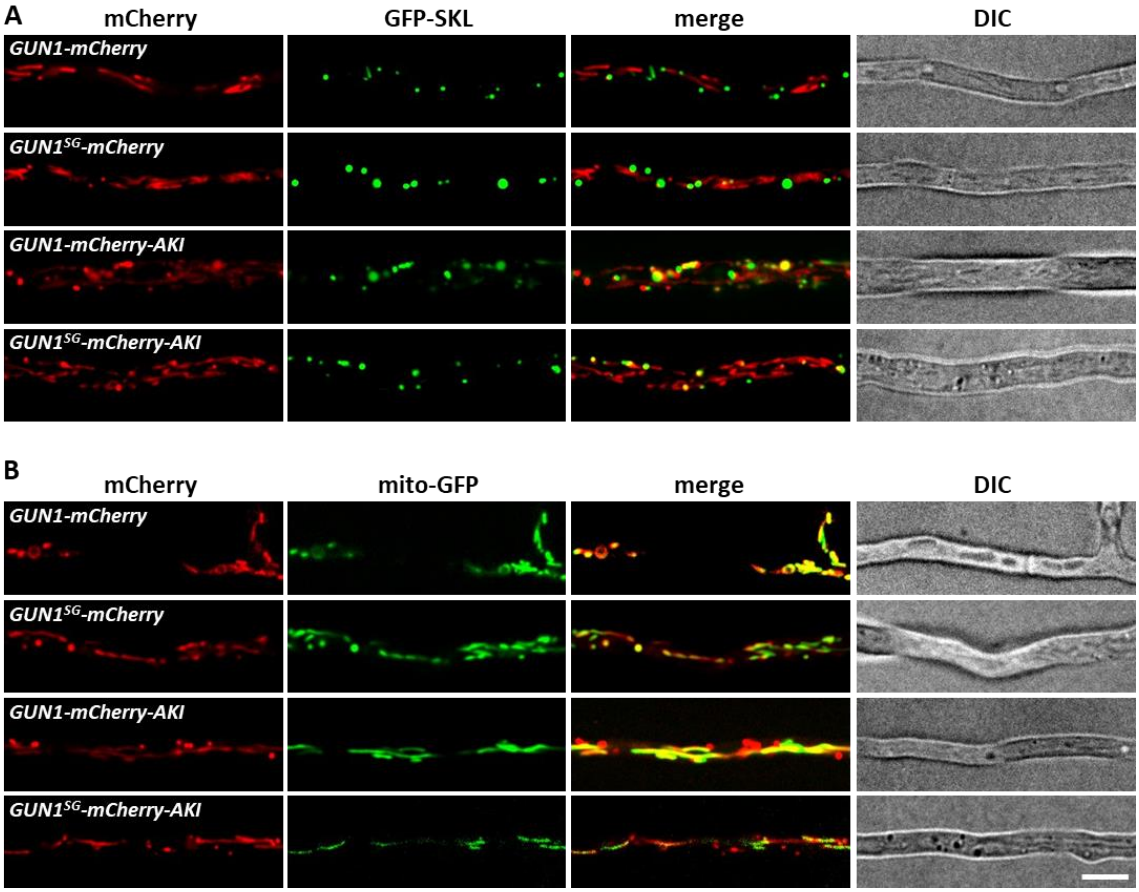

bioRxiv preprint doi: https://doi.org/10.1101/2022.04.08.487612; this version posted April 10, 2022. The copyright holder for this preprint (which was not certified by peer review) is the author/funder, who has granted bioRxiv a license to display the preprint in perpetuity. It is made available under aCC-BY-NC-ND 4.0 International license.

Fig 6: Spinning disc imaging of GUN1-mCherry-AKI and GUN1^{SG}-mCherry-AKI in ascospores

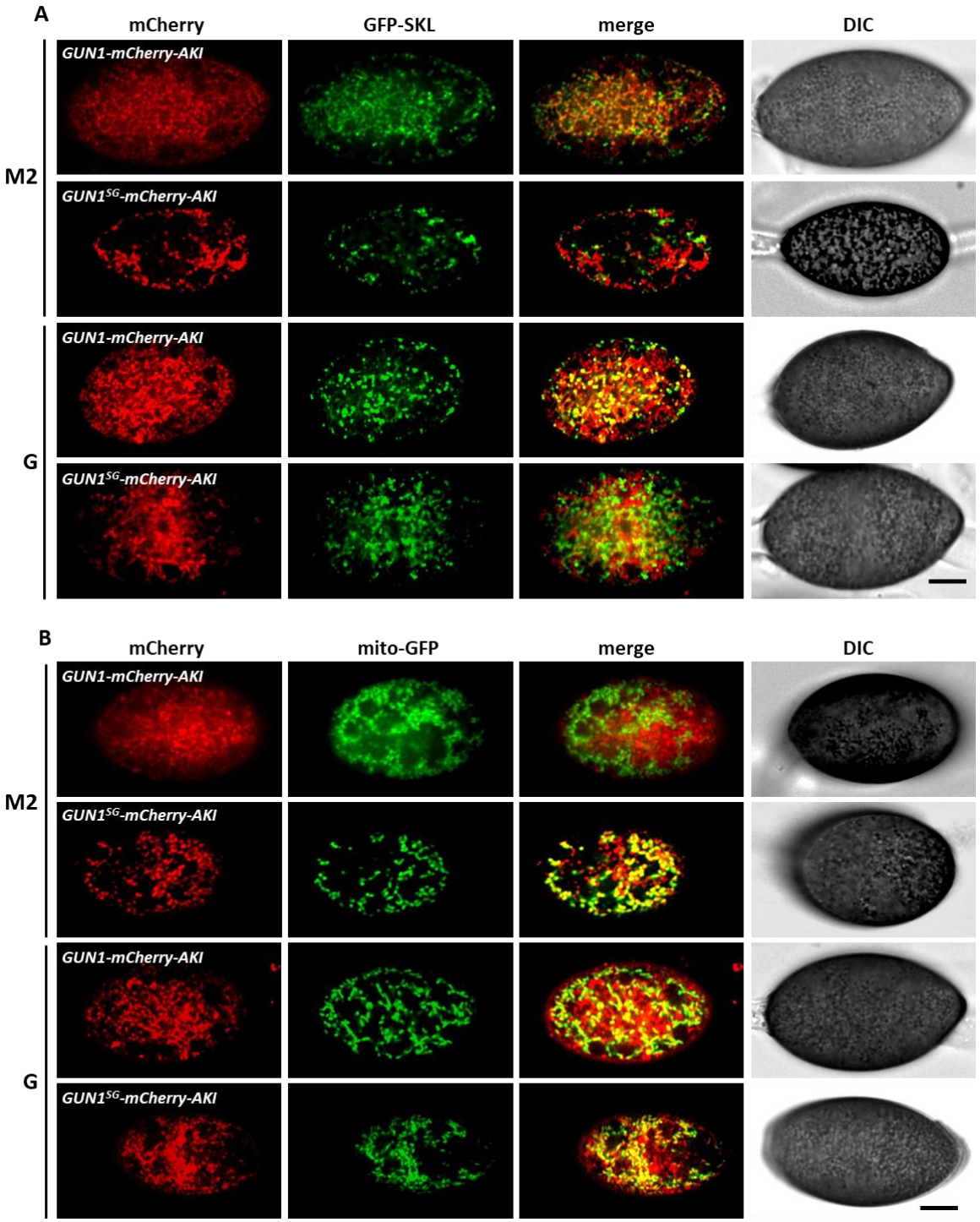

bioRxiv preprint doi: https://doi.org/10.1101/2022.04.08.487612; this version posted April 10, 2022. The copyright holder for this preprint (which was not certified by peer review) is the author/funder, who has granted bioRxiv a license to display the preprint in perpetuity. It is made available under aCC-BY-NC-ND 4.0 International license.

Fig. 7. Western blot analysis of PaMpk2 phosphorylation in ascospores

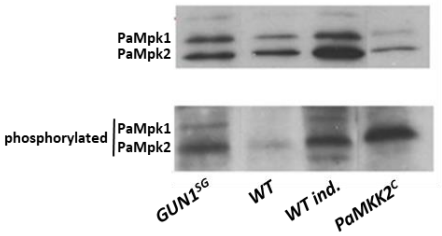

Fig.8. Regulation of ascospore germination